

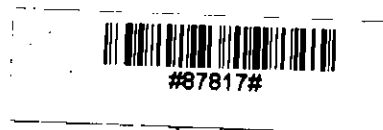
NUMERICAL SIMULATION OF BED LEVEL CHANGES OF THE GANGES

By

Md Mouludul Islam



**In partial fulfillment of the requirements for the Degree of Master of
Engineering (Water Resources).**



**DEPARTMENT OF WATER RESOURCES ENGINEERING
BANGLADESH UNIVERSITY OF ENGINEERING & TECHNOLOGY,
DHAKA, BANGLADESH.**

April, 1993

627.12095492

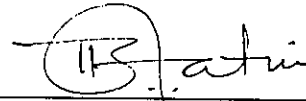
1993
MOU

BANGLADESH UNIVERSITY OF ENGINEERING AND TECHNOLOGY

DEPARTMENT OF WATER RESOURCES ENGINEERING

We hereby recommend that the project prepared by Md Mouludul Islam entitled "Numerical Simulation of the Bed Level Changes of the Ganges" be accepted as fulfilling this part of the requirements for the degree of Master of Engineering (Water Resources).

Chairman of the Committee



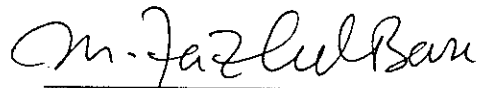
Md. Abdul Matin, Ph.D.

Member



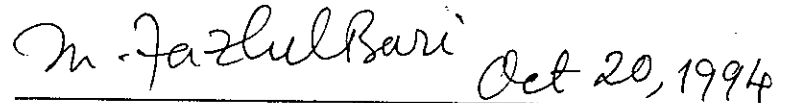
Professor Md. Abdul Halim, Ph.D.

Member



Professor M. F. Bari, Ph.D.

Head of the Department



Professor M. F. Bari, Ph.D.

April, 1993

CERTIFICATE

This is to certify that this project work has been done by me and neither this project nor any part thereof has been submitted elsewhere for the award of any degree or diploma.

Countersigned



(Dr. Md. Abdul Matin)

Signature



(Md. Mouludul Islam)

ABSTRACT

Simulation of sediment transport rate at the river Ganges and variation of bed level along the river is carried out by using a one dimensional morphological model. Non-cohesive sediment transport module of MIKE11 is used for the simulation. The upstream boundary of the model is taken at 97 km upstream of Mathabhanga offtake (Ganges 0) and downstream boundary is taken at Padma 100 km. The river system is schematized by five branches, one inflow boundary at upstream, one lateral inflow and four lateral outflow boundaries and one outflow boundary at downstream (water level boundary).

In order to make convenient for sediment calculation with hydrodynamic computation, the river is represented by equivalent cross-sectional shape and longitudinal profile. This is achieved by considering that the hydraulic properties of the representative cross-section is the same as that of the actual cross section. Simulation period is taken from April 1985 to October 1991. Simulation is carried out for hydrodynamic calibration and for transport rates. The cross-section interval varies from 2 km to 10 km in the schematization and the total length including the Padma river is 314 km. The time interval used for the morphological computation is four hours for hydrodynamic computation and four days for sediment transport computation respectively. Both for hydrodynamic and sediment transport, the results are saved after every four days.

Calibration is carried out against field observations (both water level and discharge) from 1985 to 1991. Water level comparison for simulated and observed values are taken at five key locations (Hardinge Bridge, Sengram, Mohendrapur, Baruria and Mawa) whereas discharge is compared at Baruria only. The results showed satisfactory agreement with observed values.

For morphological computation, a time series data of sediment flow is used at the upstream boundary. This time series is generated after a logarithmic transformation of observed transport rate and observed water discharges measured by BWDB. With this generated transport rates at the boundary, the sediment transport calibration is performed by comparing simulated rates. The results show very good agreement with the observed rates of sediment transport. The simulated sediment load is again verified with the loads at Hardinge Bridge as computed by various investigators.

After calibration of the model for both hydrodynamic and sediment transport, the net amount of erosion and siltation along the river reach is computed. Finally, longitudinal variation of bottom level for the monsoon season from 1988 to 1991 is drawn from the model results.

ACKNOWLEDGEMENT

I would like to express my sincere gratitude and indebtedness to Dr. Md. Abdul Matin, Assistant Professor, Department of Water Resources Engineering, Bangladesh University of Engineering and Technology for his constant guidance and supervision during the course of this study. It was a great privilege for me to work with him, whose constant guidance made it possible to conclude this project work successfully.

I would like to express my gratitude to other members of the project committee, Dr. M.F. Bari, Professor and Head, Department of Water Resources Engineering and Dr. Md. Abdul Halim, Professor, Department of Water Resources Engineering for their valuable comments, constructive criticism and suggestions regarding the work.

Special thanks are due to Mr. Shahadat Hossain, Lecturer, Institute of Flood Control and Drainage Research for his assistance.

M. Islam.

TABLE OF CONTENTS

	<u>Page</u>
Abstract	iv
Acknowledgement	vi
List of Tables	x
List of Figures	xi
List of Symbols	xiv
CHAPTER I	
INTRODUCTION	1
1.1 General	1
1.2 Objective of the Study	2
CHAPTER II	
REVIEW OF LITERATURE	3
2.1 Introduction	3
2.2 Review of Previous Studies	3
2.3 Relevant Equations for Representating Water-Sediment Motion	5
2.3.1 Continuity Equation	5
2.3.2 Momentum Equation	6
2.3.3 Sediment Continuity Equation	8
2.4 Assumptions of the Saint-Venant Equation	9
2.5 Description of the Flow Resistance	9
2.6 Solution Technique	11
2.6.1 Abbott's Implicit Scheme	11

TABLE OF CONTENTS (CONT.)

	<u>Page</u>
2.6.2 The Double Sweep Algorithm	17
2.7 Solution Method	19
CHAPTER III	
APPLICATION OF THE MORPHOLOGICAL MODULE	21
3.1 Introduction	21
3.2 Sediment Transport Equations	22
3.3 Methods of Simulation	24
3.3.1 The Explicit Sediment Transport Models	25
3.3.2 Morphological Model	28
3.4 Flow Resistance Relationship	29
CHAPTER IV	
SIMULATION OF BED LEVEL CHANGES	33
4.1 Introduction	33
4.2 Data Collection and Processing	33
4.2.1 Topographic Data	34
4.2.2 Discharge Data	35
4.2.2.1 Discharge Hydrograph of the Ganges	35
4.2.3 Water Level Data	36
4.2.4 Sediment Data	36
4.2.4.1 Analysis of Sediment Load	37
4.2.4.2 Selection of Representative Grain Size	38

TABLE OF CONTENTS (CONT.)

	<u>Page</u>
4.3 Sediment Transport Model Set Up	38
4.3.1 Basis for Schematization	39
4.4 Conveyance Analysis of the Ganges Reach	41
4.5 Hydrodynamic Schematization	42
4.6 Boundary Conditions	43
CHAPTER V	
RESULTS AND DISCUSSION	45
5.1 Hydrodynamic Calibration of the Model	45
5.2 Sediment Transport Model	45
5.3 Model Run	46
5.3.1 Calibration of Sediment Transport Model	46
5.3.2 Model Results and Analysis	47
5.4 Distribution of Runoff and Sediment Load	48
5.5 The Statistical Parameter of the Sediment Load	48
5.6 Bed Level Variation of the River Ganges	49
CHAPTER VI	
SUMMARY AND CONCLUSIONS	75
6.1 Summary	75
6.2 Conclusions	76
6.3 Recommendations	77
REFERENCES	78

LIST OF TABLES

		<u>Page</u>
Table 4.1	Rating Parameters at Harding Bridge	50
Table 4.2	Correlation Coefficient for the Sediment Transport Rates and Discharge	51
Table 5.1	Grain Diameters Used in the Model	51
Table 5.2	Computed Annual Flow and Sediment Load at Hardinge Bridge	51
Table 5.3	Comparison of Annual Sediment Load	52
Table 5.4	Percentage of Monthly Runoff and Sediment Load (1985-1991)	52
Table 5.5	Distribution of Runoff and Sediment Load (July-Sept.)	52
Table 5.6	Statistical Parameters of the Computed Annual Sediment Load.	52

LIST OF FIGURES

		Page
Figure 2.1	The Elementary Control Volume in One Dimensional Flow	5
Figure 2.2	Definition Sketch of Sediment Continuity Equation	8
Figure 2.3	Effective Flow Area Concept	10
Figure 2.4	Centering of Continuity Equation in 6-Point Abbott-Scheme	11
Figure 2.5	River Bed Representation in Abbott's Scheme	12
Figure 2.6	Discretization in Abbott's Scheme	13
Figure 2.7	Centering of Momentum Equation in 6-Point Abbott-Scheme	14
Figure 2.8	Grid in Simple Systems of Channels	19
Figure 2.9	Double Sweep Algorithm	20
Figure 3.1	Representation of an Explicit Scheme	25
Figure 3.2	Representation of an Implicit Scheme	26
Figure 3.3	Flow Resistance, θ - θ' Relationship	29
Figure 3.4	Flow over a Dune Covered Bed	31
Figure 4.1	Comparison of The Generated Discharge Hydrograph at Hardinge Bridge	53
Figure 4.2	Sediment Rating Curve at Hardinge Bridge (1966-'70)	54
Figure 4.3	Sediment Rating Curve at Hardinge Bridge (1976-'89)	55

LIST OF FIGURES (CONT.)

	Page
Figure 4.4 Sediment Rating Curve at Hardinge Bridge (1966-'89)	56
Figure 4.5 Generated Sediment and Discharge Hydrograph at Hardinge Bridge	57
Figure 4.6 Equi Conveyance Profiles for the River Ganges (1988-'89)	58
Figure 4.7 Equi Conveyance Profiles for the River Ganges (1990-'91)	59
Figure 4.8 Model Conveyance Curve (1988-'89)	60
Figure 4.9 Cross-Sectional Area vs Normalized Water Level (1988-'89)	61
Figure 4.10.a Idealized Cross Section of the River Ganges	62
Figure 4.10.b Conveyance vs Waterlevel Curve for Idealized Section	62
Figure 4.10.c Area vs Water Level Curve for Idealized Section	63
Figure 4.10.d Hydraulic Radius vs Water Level Curve of the Idealized Section	63
Figure 4.10.e Width vs Water Level Curve of the Idealized Section	64
Figure 4.10.f Resistance Factor vs Water Level of the Idealized Section	64
Figure 4.11 Equi Conveyance Profiles at Bankfull Conveyance (1988-'89 and 1990-'91) of the River Ganges	65
Figure 4.12 Scheme Plane of the Model	66
Figure 5.1 Calibration of the Hydrodynamic Model at the Ganges (Water level)	67

LIST OF FIGURES (CONT.)

	Page
Figure 5.2 Calibration of the Hydrodynamic Model at Padma (Water Level and Discharge)	68
Figure 5.3 Computed Sediment Transport Rate for the Ganges	69
Figure 5.4 Observed and Simulated Sediment Hydrographs at Hardinge Bridge	70
Figure 5.5 Comparison of Simulated and Observed Transport Rate (1990-'91)	70
Figure 5.6 Variation of Annual Discharge and Total Load at Hardinge Bridge	71
Figure 5.7 Distribution of Degradation and Aggradation Along the Ganges	72
Figure 5.8 Variation of Bed Level at Harding Bridge, Sengram and Mohendrapur (1985-'91)	73
Figure 5.9 Variation of Bed Level Along the River Reach.	74

LIST OF SYMBOLS

a	=	Reference level in calculation of suspended load
A	=	Cross Sectional area
b_s	=	Width of river section with flood plain
C	=	Chezy's co-efficient
d	=	Mean grain size of the bed material
D	=	Boundary layer thickness
f	=	Function
g	=	Acceleration due to gravity
h	=	Water elevation
q	=	Flow discharge per unit width
h_j^n	=	Water depth
K	=	Equivalent load roughness
M	=	Manning's co-efficient
n	=	Time step between the core grid
Q	=	Flow Discharge
Q_j^n	=	Flow discharge at grid j & time interval n
q_s	=	Suspended Sediment load transport rate
q_t	=	Total transport rate
R	=	Resistance radius
R_h	=	Hydraulic radius
S	=	Relative density of bed material

LIST OF SYMBOLS (Contd.)

u_f	=	Bed shear velocity or friction velocity
V	=	Mean flow velocity
V_g	=	Bed shear velocity related to the grains
W	=	Width of river channel
Z	=	Bottom level above datum
α	=	Energy co-efficient
β	=	Momentum co-efficient
γ_s	=	Unit weight of sand
Δt	=	Time step
Δx	=	Space step
θ	=	Dimensionless bed shear stress
θ'	=	Dimensionless skin friction
ρ	=	Fluid density
τ	=	Bed shear stress
τ'	=	Skin friction
τ''	=	Form friction
ϕ	=	Dimensionless sediment transport rate

CHAPTER I

INTRODUCTION

1.1 General

The behavior of a natural river is affected by both sediment and discharge flow characteristics, physical controls in a river reach, upstream control of a river and distribution of grain size in the river. Problems involving sediment movement in a river resulting from various causes are numerous and of great extent. Construction of flood embankment causes increased flooding downstream or may cause changes in sedimentation characteristics in the river reach. There is a difficulty in predicting and quantifying these effects, it is necessary to predict the continually changing configuration of river morphology. Changes of bed level variation under such circumstances extend over a long period of time and is of great importance.

The hydraulic resistance of alluvial rivers depends mainly on the size of sand dunes on the river bed. The larger and steeper the dunes are the larger is the hydraulic resistance. Generally, with the increase of bed load, sand dunes grow and length of the dunes increases but the height of the dunes decreases when suspended load become dominant. Hence, with the increasing discharge, the hydraulic resistance will first increase and later decrease as the suspended load increases. Hence, it becomes essential to study the effect of the large scale movement of the sediment on river bed levels.

Numerical hydrodynamic models of unsteady flow in rivers are widely used as an engineering tool in the design and planning of water resources projects. In recent years, several studies viz Master Plan Organization (MPO, 1987), Bangladesh Water Development Board (BWDB, 1987), used the hydrodynamic as well as morphological models of unsteady flow for computing flood flows and transport rates for the rivers in Bangladesh. In recent time one of the most widely used modelling tool in application in Bangladesh is MIKE11 which is developed by Danish Hydraulic Institute (DHI).

1.2 Objective of the study

Owing to the geographical location of Bangladesh, about 93% of the total streamflow with huge sediment load originating in the upstream catchments in India, Nepal, Bhutan and China passes through the country. Bangladesh through its great river systems of the region, like other major rivers the Ganges drains the dominant part of sediment load. A large amount of siltation takes place every year in the river reach resulting the bed level changes.

Using the hydrodynamic and morphological model, an attempt has been made to simulate the mean bed level changes of the river Ganges. Thus the following objectives have been set:

- a. To simulate the sediment transport rate of key station i.e. Hardinge Bridge of the river Ganges.
- b. To simulate the variation of mean bed level of a selected reach of the river under study.

CHAPTER II

REVIEW OF LITERATURE

2.1 Introduction

A brief review of various earlier studies will be made in this chapter. In addition, the description of relevant equations and the solution methods utilised in this study will be briefly illustrated.

2.2 Review of previous studies

In recent years several studies on morphological changes of major rivers in Bangladesh have been made. Analysis of the sedimentation and hydraulic characteristics of the Jamuna has been done by Coleman (1969). Dad (1977) had studied the shifting Pattern of the Ganges river based on the plan map of the banklines. According to Dad (1977), the shifting of thalweg is due to movement of sand bars, mid-islands and due to aggradation. Rahman (1978) had studied the erosion of the Padma river from Goalunda to confluence of Padma-Meghna near Chandpur. He produced some relationships between thalweg sinuosity with meander pattern. Habibullah (1985) analysed the cross-sections of Jamuna and determined the bed level variations between the years 1965-66 and 1983-84 for the reach Aricha to Charnatua. Hossain (1991) reanalysed the bed level variation of the Jamuna for the above reach utilising recent data of 1985-86. SPARRSO has been collecting the spot images of the rivers using remote sensing techniques to the river morphology.

Using the historical maps on the river Ganges, Chowdhury (1986) conducted some studies on the shifting pattern of the river.

Using these sediment data in the Ganges at Kalikapur an analysis has been made by Bari (1978) for the period 1970, 1972 and 1973. He established rating curves for the Ganges at this section and recommended that Colby and Engelund-Hansen formulas yield a result which is more close to the measured value. Alam and Ahmed (1980) have also analysed the sediment data at the same station by using various transport equations for the period 1969 to 1972. According to them, Colby's equation was found to be good in comparison with the measured sediment flow.

Nahar (1990) developed a numerical model to calculate the change of mean bed level at different locations of Jamuna. The China-Bangladesh joint expert team (CBJET, 1991) studied the behaviour of the confluence of the Brahmaputra and the Ganges river.

Hossain (1989) found that the net deposition in the Ganges upto Brahmaputra confluence was approximately $4.26 \times 10^8 \text{ m}^3$ during 1967-68 to 1979-80 which corresponds to about 4.30 cm sediment deposition each year throughout the reach. However, according to CBJET (1991), the annual suspended sediment flow through the Ganges varies from 181×10^6 to 304×10^6 tons, The total annual sediment load at Hardinge Bridge varies from 220×10^6 to 368×10^6 tons.

The excess sediment supply may change the river pattern, reduce the conveyance and in this aspects it is important to study the aggradation and degradation of the river bed. With the artificial changes of the width of the river at some locations such as at Hardinge Bridge constriction and for surface water requirements, it is necessary to know the morphological behaviour of the rivers particularly bed level variation due to siltation and erosion. In this study, attempts has been made to focus the river morphology in connection with the effect of the river bed and peak flow levels at key locations of the river Ganges due to increase and decrease of sediment, increase of dominant discharge etc.

2.3 Relevant equations for representing water-sediment motion

2.3.1 Continuity equation

Conservation of mass for a control volume states the net flow into the control volume equals the net storage change in the control volume. In Figure 2.1 a control volume is shown. Where, x is the direction of flow.

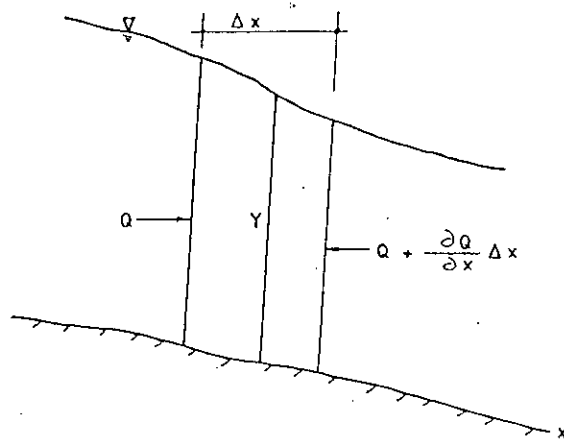


Figure 2.1 The elementary control volume in one dimensional flow

According to Figure 2.1 mass conservation equation yields

$$\frac{\partial Q}{\partial X} + \frac{\partial A}{\partial t} = 0 \quad (2.1)$$

If the channel storage width is b_s , depth of flow is h and the lateral flow into the system is q , then the equation of continuity becomes:

$$\frac{\partial Q}{\partial x} + b_s \frac{\partial h}{\partial t} = q \quad (2.2)$$

In which, the term $\frac{\partial h}{\partial t}$ expresses the rate of change of water surface elevation caused by the storage in the constant volume and $\frac{\partial Q}{\partial x}$ expresses the rate of change of discharge in the control volume.

2.3.2 Momentum equation

Conservation of momentum states that the rate of momentum entering into the element plus the sum of the forces acting on the element is equal to the rate of accumulation of momentum inside the element. The rate of momentum flow in a fluid mass is the product of the mass of flow and velocity.

Considering force due to gravity, pressure, frictional resistance and channel geometry (either narrow or wide) on a fluid mass the momentum equation becomes:

$$\frac{\partial Q}{\partial t} + \frac{\partial}{\partial x} \left(\frac{Q^2}{A} \right) + gA \frac{\partial h}{\partial x} + gAS_f = 0 \quad (2.3)$$

For non-uniform velocity distribution over the cross-section momentum correction factor β is introduced and from Manning formula

$$S_f = \frac{n^2 Q^2}{A^2 R^{4/3}}$$

We have,

$$\frac{\partial Q}{\partial t} + \frac{\partial}{\partial x} \left(\beta \frac{Q^2}{A} \right) + gA \frac{\partial h}{\partial x} + \frac{gn^2 Q|Q|}{AR^{4/3}} = 0 \quad (2.4)$$

If lateral inflow is considered and u_g is its downstream velocity component, then equation 2.4 becomes

$$\frac{\partial Q}{\partial t} + \frac{\partial}{\partial x} \left(\alpha \frac{Q^2}{A} \right) + gA \frac{\partial h}{\partial x} + \frac{gn^2 Q|Q|}{AR_h^{4/3}} - \left(u_g - \frac{Q}{A} \right) q = 0 \quad (2.5)$$

Equations 2.2 and 2.5 are known as the Saint Venant equations.

2.3.3 Sediment continuity equation

The dependent variables for the sediment continuity equation are (i) flow velocity $u(x,t)$, (ii) sediment transport $q_s(x,t)$, (iii) water depth $a(x,t)$ and (iv) bed level $z(x,t)$.

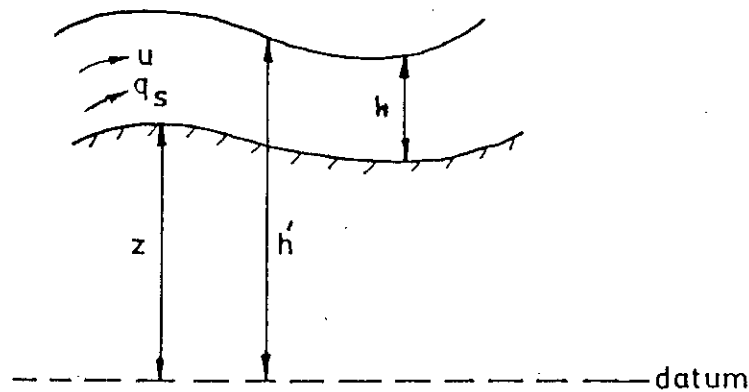


Fig.2.2 Definition sketch

In some cases water level $h' = z + h$ will be considered. The width of the river $B(x,t)$ is supposed to be known. Considering the constant width leads to the possibility of taking the basic equation for the unit width. The basic sediment continuity equation per unit width can be represented by

$$\frac{\partial z}{\partial t} + \frac{\partial q_s}{\partial x} = 0 \quad (2.6)$$

Here $q_s = f(u, \text{roughness parameters, etc})$

where, $\frac{\partial z}{\partial t}$ = Change in bottom level with respect to time.

$\frac{\partial q_s}{\partial x}$ = Change in transport rate per unit width with respect to space.

2.4 Assumptions of the Saint-Venant equations

The Saint-Venant equations for unsteady flow (equations 2.2 and 2.5) are based upon the following assumptions:

- i) The flow is one-dimensional i.e. the velocity is uniform over the cross-section and water level across the section is horizontal.
- ii) The streamline curvature is small and vertical acceleration is negligible, hence the pressure is hydrostatic.
- iii) The effects of boundary friction and turbulence can be accounted for through resistance laws analogous to those used for steady-state flow.
- iv) The average channel bed slope is small so that the cosine of the angle it makes with the horizontal is replaced by unity.

2.5 Description of the flow resistance

Bed resistance can be described in two different ways, the Chezy description and the Manning description.

Following the Chezy description, the reduced momentum due to resistance will be described as:

$$\tau_r = \frac{gQ|Q|}{C^2AR_h} \quad (2.7)$$

where C is the Chezy coefficient.

Following the Manning description, the similar term becomes:

$$\tau_r = \frac{gQ|Q|}{M^2AR_h^{4/3}} \quad (2.8)$$

where M is the Manning number.

Both Chezy and Manning coefficient can be described as depth dependent functions.

The resistance to flow on the flood plains will generally be higher than in the rivers and khals, because of the irregular surface and vegetation. This is accounted for in the model by the "effective flow area" concept. Following this concept, the flow contributions from different areas of the cross section are reduced by a factor inversely proportional to the increase in resistance. This affects both the integrated cross-sectional area and the resistance radius and they are in this way brought into the resistance term in the momentum equation.

The concept of effective flow area is shown for a schematized example in Figure 2.3.

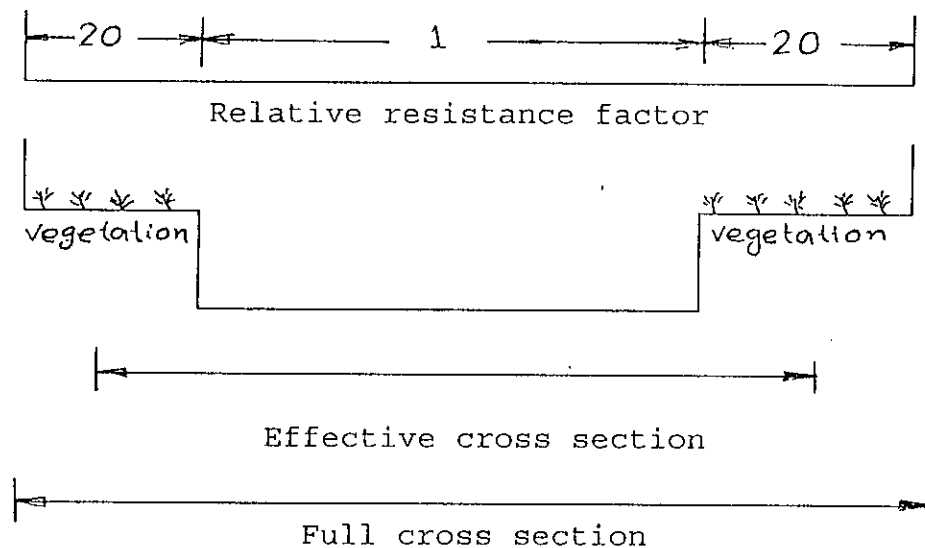


Figure 2.3 Effective flow area concept.

2.6 Solution technique

2.6.1 Abbott's implicit scheme

The scheme was developed by Abbott (1975) at the Delft University of Technology, the Netherlands. The scheme uses a different form of the flow equations than those usually derived. This is due to the distinction made between the "storage width" in the continuity equation and the so called "computational" or "mathematical" width used in the dynamic equation.

The adopted numerical scheme is a 6-point Abbott-scheme as shown in Figure 2.4

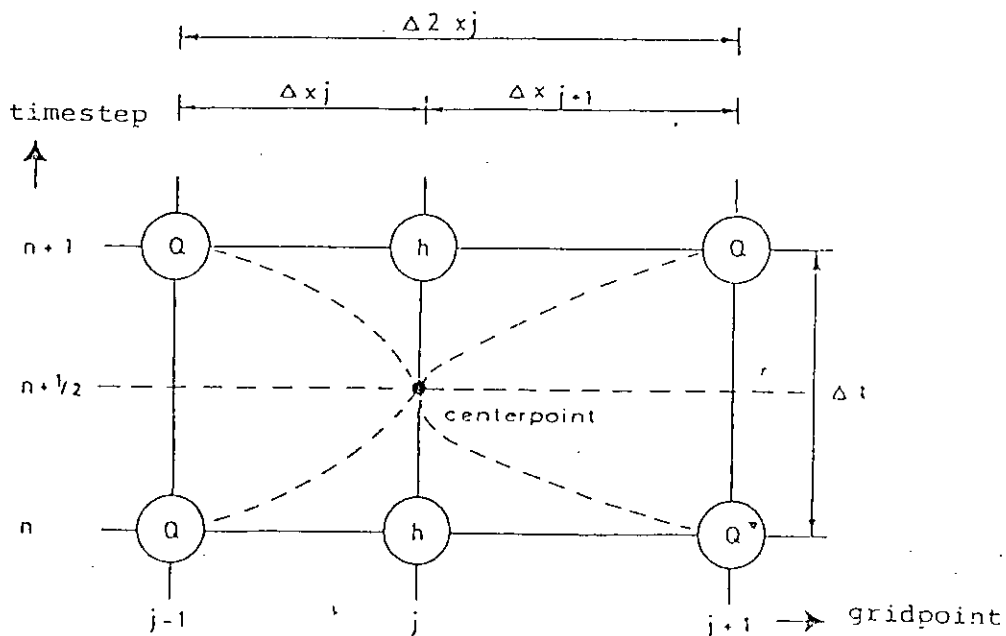


Figure 2.4 Centering of continuity equation in 6-point Abbott-scheme.

The dynamic equation has the following form:

$$\frac{\partial Q}{\partial t} + \frac{\partial}{\partial x} \left(\frac{\alpha Q^2}{A} \right) + gA \frac{\partial h}{\partial x} + \frac{gQ|Q|}{C^2 AR_h} = 0 \quad (2.9)$$

$$\alpha = \frac{A}{Q^2} \int Au^2 dA$$

One can write

$$\frac{\partial}{\partial x} \left(\alpha \frac{Q^2}{A} \right) = \frac{2\alpha Q}{A} \frac{\partial Q}{\partial x} - \frac{\alpha Q^2}{A^2} \frac{\partial A}{\partial x} + \frac{Q^2}{A} \frac{\partial \alpha}{\partial x} \quad (2.10)$$

Where,

$$\frac{\partial Q}{\partial X} = \frac{-B_s \partial h}{\partial t}$$

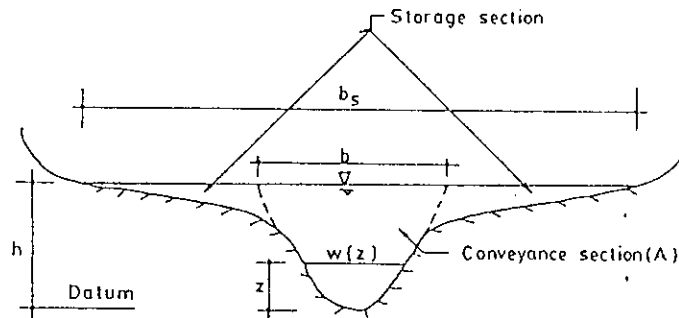


Figure 2.5 River bed representation in Abbott's scheme.

Referring to Figure 2.5 and introducing a mathematical width B such that

$$\frac{\partial A}{\partial x} = B \frac{\partial h}{\partial x} + h \frac{dB}{dh} \frac{\partial h}{\partial x} \quad (2.11)$$

and substituting equation 2.10 and 2.11 into equation 2.9 gives

$$\frac{\partial Q}{\partial t} - \frac{2\alpha QB_s}{A} \frac{\partial h}{\partial t} - \left[\frac{\alpha Q^2}{A^2} (B+h) \frac{dB}{dh} - gA + \frac{Q^2}{A} \frac{d\alpha}{dh} \right] \frac{\partial h}{\partial x} + \frac{gQ|Q|}{C^2 AR_h} = 0 \quad (2.12)$$

The discretization according to a special finite difference implicit scheme is applied to equations 2.1 and 2.2. The scheme is described below with reference to the (x,t)-plane in Figure 2.6.

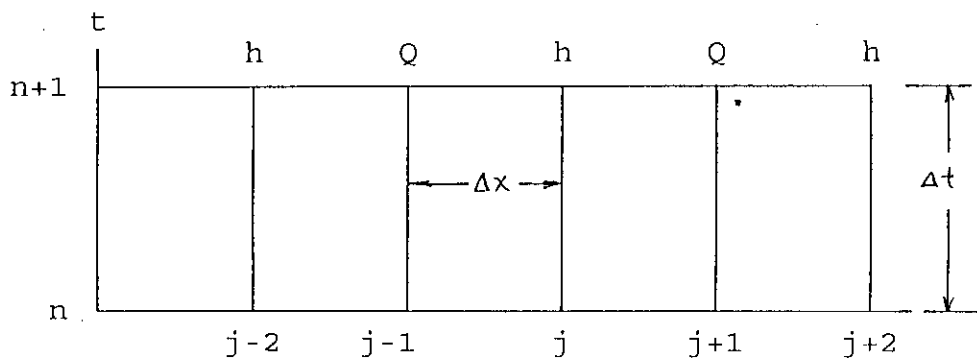


Figure 2.6 Discretization in Abbott's scheme.

Discharges Q and depth h are not computed at the same points. Thus the depths may be computed at all even points $j = 0, 2, \dots$, while the discharges are computed at all odd points $j = 1, 3, \dots$. The discretization proceeds as follows:

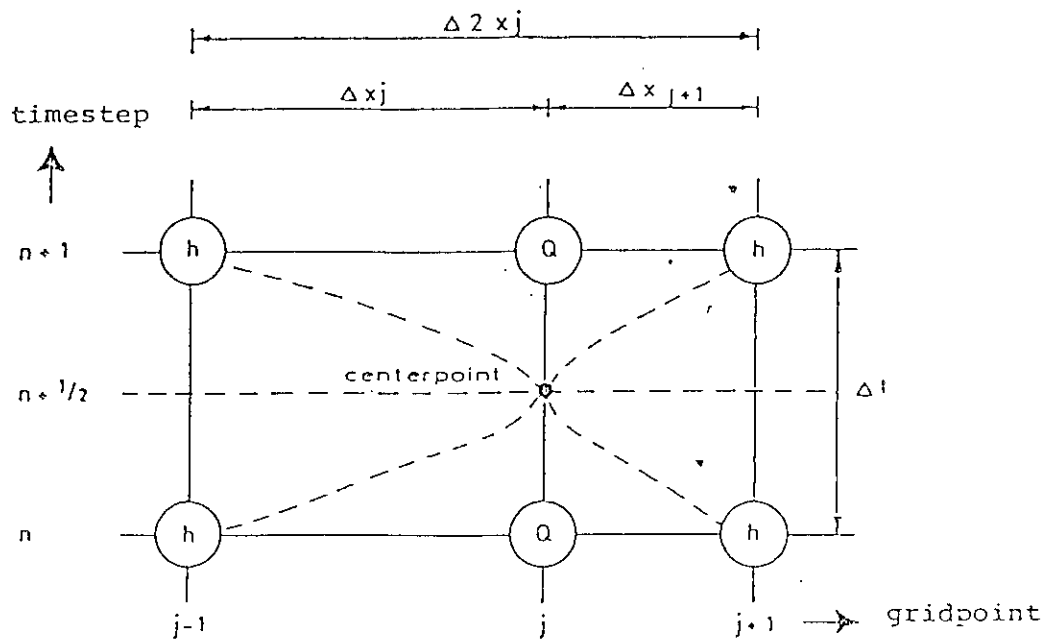


Figure 2.7 Centering of momentum equation in 6-point Abbott-scheme.

(i) continuity equation

$$\frac{\partial Q}{\partial x} \approx \frac{1}{X_{j+1} - X_{j-1}} \left[\frac{1}{2}(Q_{j+1}^n + Q_{j+1}^{n+1}) - \frac{1}{2}(Q_{j-1}^n + Q_{j-1}^{n+1}) \right]$$

$$\frac{\partial h}{\partial t} \approx \frac{1}{\Delta t} (h_j^{n+1} - h_j^n)$$

$$D_1 \frac{h_j^{n+1} - h_j^n}{\Delta t} + \frac{1}{2(X_{j+1} - X_{j-1})} [(Q_{j+1}^n + Q_{j+1}^{n+1}) - (Q_{j-1}^n + Q_{j-1}^{n+1})] = 0$$

(2.13)

where $D_1 = B_s$.

(ii) Dynamic equation

$$\frac{\partial Q}{\partial t} \approx \frac{1}{\Delta t} (Q_{j-1}^{n+1} - Q_{j-1}^n) ;$$

$$\frac{\partial h}{\partial t} \approx \frac{1}{\Delta t} \left[\frac{X_j - X_{j-1}}{X_j - X_{j-2}} (h_{j-2}^{n+1} - h_{j-2}^n) + \frac{X_{j-1} - X_{j-2}}{X_j - X_{j-2}} (h_j^{n+1} - h_j^n) \right] ;$$

$$\frac{\partial h}{\partial x} \approx \frac{1}{X_j - X_{j-2}} - \left[\frac{1}{2} (h_j^n + h_j^{n+1}) - \frac{1}{2} (h_{j-2}^n + h_{j-2}^{n+1}) \right] ;$$

$$Q|Q| \approx |Q_{j-1}^n| Q_{j-1}^{n+1}$$

Using these formulas Equation 2.12 may be written as:

$$\begin{aligned} & \frac{Q_{j-1}^{n+1} - Q_{j-1}^n}{\Delta t} - D_2 \frac{1}{\Delta t} \left[\frac{X_j - X_{j-1}}{X_j - X_{j-2}} (h_{j-2}^{n+1} - h_{j-2}^n) + \frac{X_{j-1} - X_{j-2}}{X_j - X_{j-2}} (h_j^{n+1} - h_j^n) \right] \\ & - D_3 \frac{1}{2(X_j - X_{j-2})} [(h_j^n + h_j^{n+1}) - (h_{j-2}^n + h_{j-2}^{n+1})] + D_4 |Q_{j-1}^n| Q_{j-1}^{n+1} = 0 \end{aligned} \quad (2.14)$$

where

$$\begin{aligned} D_2 &= \frac{2\alpha Q B_s}{A}, \quad D_3 = \frac{\alpha Q^2}{A^2} \left(b_m + h \frac{dB_m}{dh} \right) - gA + \frac{Q^2}{A} \frac{d\alpha}{dh} \\ D_4 &= \frac{g}{C^2 A R_h} \end{aligned} \quad (2.15)$$

With the equation 2.13 written in this way, an important question arises as to where in the (x,t) - plane should the values of coefficients D_1, D_2, D_3 and D_4 be taken. If they are evaluated at time level $t_n = n\Delta t$, they are known. According to Abbott's method, however, these coefficients are evaluated at the center points of the mesh, at time $t = (n+1/2)\Delta t$. Consequently the following steps are necessary to solve the equations:

1. Evaluate coefficients D_1, D_2, D_3 and D_4 at time $t_n = n\Delta t$.
2. Write equation 2.13 and 2.14 in the form

$$\alpha_j Q_{j+1}^{n+1} + \beta_j h_j^{n+1} + \gamma_j Q_{j-1}^{n+1} = \delta_j$$

$$\alpha_j^* Q_{j+1}^{n+1} + \beta_j^* h_j^{n+1} + \gamma_j^* Q_{j-1}^{n+1} = \delta_j^* \quad (2.16)$$

where coefficients α_j, β_j , etc. are known functions of D_1, D_2, D_3, D_4 and the other variables are known at time $T_n = n\Delta t$.

3. Solve the system of equation 2.16 by the double sweep algorithm as described later.

4. Evaluate D_1, D_2, D_3 and D_4 with time level $t = (n+1/2)\Delta t$ as functions of h^n, Q^n and the new values h^{n+1}, Q^{n+1} found in step (3).

5. Compare the new values of coefficients D_1, D_2, D_3 and D_4 with the previous estimate and if the differences are too great go back to step (2) using these new values to evaluate $\alpha_j, \beta_j \dots$ etc.

2.6.2 The double sweep algorithm

The continuity equation and the momentum equation can be formulated in a similar form. Using instead of h and Q , the general variable name Z which thus becomes h in grid points with odd numbers and Q in grid points with even numbers, the general formulation will be:

$$A_j Z_{j-1}^{n+1} + B_j Z_j^{n+1} + C_j Z_{j+1}^{n+1} = D_j \quad (2.17)$$

Introducing a set of quasi-constants, E_j , and F_j , relating each unknown to the set of unknown in the neighboring point

$$Z_{j-1}^{n+1} = E_j Z_j^{n+1} + F_j \quad (2.18)$$

and substituting equation 2.18 into equation 2.17 gives

$$A_j E_j Z_j^{n+1} + B_j Z_j^{n+1} + C_j Z_{j+1}^{n+1} = D_j - A_j F_j$$

or

$$Z_j^{n+1} = \frac{-C_j}{B_j + A_j E_j} Z_{j+1}^{n+1} + \frac{D_j - A_j F_j}{B_j + A_j E_j}$$

By analogy

$$E_j = \frac{-C_{j-1}}{B_{j-1} + A_{j-1} E_{j-1}} \quad (2.19)$$

$$F_j = \frac{D_{j-1} - A_{j-1} F_{j-1}}{B_{j-1} + A_{j-1} E_{j-1}} \quad (2.20)$$

The complete set of equations for a system of N grid points having R external boundaries will provide N-R linear equations of the general form of equation 2.18. At the boundaries another R known values or unknown relations between the independent variables will form the missing R equations.

At the first grid point values for E and F follow from the boundary condition which can be either a relation between Q and h or Q or h given directly. From these starting values and with successive use of equation 2.19 and 2.20 for every grid point along the channel, E_j and F_j can be determined for every grid point. This is called the EF-sweep.

Arriving at the last grid point the boundary condition there is used to initiate "double sweep" algorithm, where all the unknowns, h and Q, are evaluated by successive use of equation 2.18. This is called the HQ - sweep. In this way, one computational cycle is carried through. The cycle is then repeated with more accurate values for the coefficient in equation 2.17 until the desired accuracy is obtained. A new set of external and internal conditions will now define the next cycle.

2.7 Solution method

The model solves the vertically integrated equations of conservation of volume and momentum (i.e. the Saint Venant equations) :

Conservation of volume:

$$\frac{\partial Q}{\partial x} + b \frac{\partial h}{\partial t} = q \quad (2.21)$$

Conservation of momentum:

$$\frac{\partial Q}{\partial t} + \frac{\partial}{\partial x} (\beta Q^2 / A) + gA \frac{\partial h}{\partial x} + \frac{gQ|Q|}{C^2 AR} = 0 \quad (2.22)$$

For nodal points a special mass conservation equation is derived. As the compatibility condition at the nodal points, the water levels for the connecting branches are set equal.

The equations are solved by Crank Nicolson implicit finite difference technique with variables defined on a staggered grid as shown in Figure 2.8.

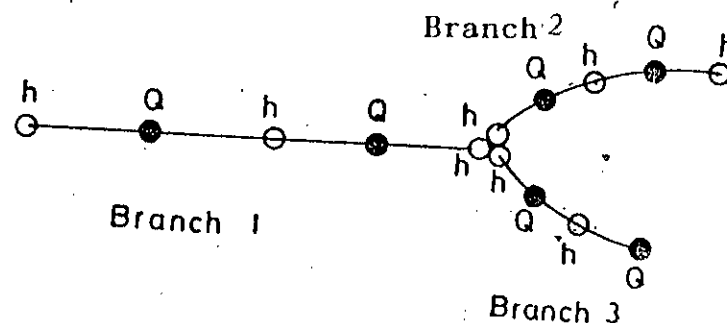


Figure 2.8 Grid in simple systems of channels.

The grid is generated by the system automatically, based on the available topography, the user specified grid points (bridges, weirs, narrow cross-sections) and the maximum space step in the river definition. The water levels h and the discharges Q are calculated alternating along the branches.

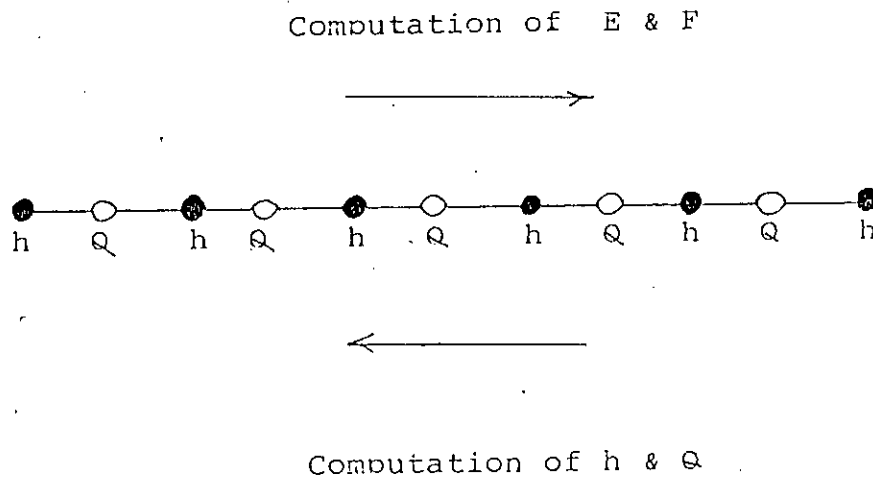


Figure 2.9 Double sweep algorithm.

For the solution, the double sweep method is used by sweeping from one boundary to the other, computing co-efficients E and F and sweeping backwards computing h and Q . This is schematized for a single branch in Figure 2.9.

A general solution procedure has been incorporated in MIKE11 which solves the equations for arbitrary channel networks by solving the nodal point co-efficient matrix.

CHAPTER III

APPLICATION OF THE MORPHOLOGICAL MODULE

3.1 Introduction

The one-dimensional morphological modelling package is an integrated part of MIKE11, which is used for the one-dimensional hydrodynamic modelling developed at the Technical University of Denmark for the hydrodynamic simulation of unsteady one dimensional flows assuming vertically homogeneous fluids. Input data are the bathymetry and the relevant hydraulic conditions (resistance coefficient, momentum distribution coefficient, hydrographic boundary conditions etc.). This model can be applied for

- tidal exchange study
- flow routing study
- Irrigation and water resources study
- reservoir study
- flow investigation in harbour

The model is also especially designed to execute morphological models.

The morphological model calculates the sediment transport capacity and alluvial resistance on the basis of hydraulic conditions calculated using output from the hydrodynamic model with time and space domain. The non-cohesive sediment transport capacity can be computed together with accumulated erosion/sedimentation rates through several different transport models.

3.2. Sediment transport equations

Four sediment transport equations are incorporated in MIKE11 for the calculation of sediment transport capacity and alluvial roughness. The salient features of these equations can be summarized as follows:

(1) Engelund-Hansen formula

Engelund-Hansen (1967) formula is one of the simplest way of computing the total sediment load. The important input for the use of this equation is the median sediment size (D_{50}) of the bed material. Use of this formula provides the sediment transport rate and consequent accumulated erosion/siltation of the bottom level.

Engelund and Hansen (1967) developed this sediment discharge formula which was based on data from experiments in a specific series of tests in a large flume. The sediments used in this flume had median fall diameters of 0.19 mm, 0.27 mm, 0.45 mm and 0.93 mm.

According to Engelund - Hansen

$$f_e \phi_e = 0.1 \tau_*^{5/2} \quad (3.1)$$

where

$$f_e = 2 \frac{\tau_o}{\rho \gamma^2} = \frac{2gd_s}{\gamma^2} \quad (3.2)$$

$$\phi_e = \frac{g_s}{\gamma_s \sqrt{\left(\frac{\gamma_s}{\gamma} - 1\right) g d_{50}^3}} \quad (3.3)$$

$$\tau_* = \frac{\tau_o}{(\gamma_s - \gamma) d_{50}} \quad (3.4)$$

Eliminating f_e , ϕ_e and τ_* from equation 3.1 gives

$$q_t = 0.05 \gamma_s V^2 \sqrt{\frac{d_{50}}{g \left(\frac{\gamma_s}{\gamma} - 1\right)}} \left[\frac{\tau_o}{(\gamma_s - \gamma) d_{50}} \right]^{3/2} \quad (3.5)$$

Since the equation is dimensionally homogeneous it can be used with any consistent set of units.

(2) The Ackers & White equation

This is a semi-empirical sediment transport equation which is partly based on dimensional analysis but physical argument had been used to derive the form of the functions that were tested. It calculates total transport rate and input requires the bed material sizes of D_{35} and D_{65} . It gives the results in the form of (i) Sediment transport (ii) Accumulated erosion /sedimentation (iii) bottom level.

(3) The Engelund and Fredsoe equation .

The sediment transport formula presented by Engelund and Fredsoe (1976) is developed considering the dune bed form. It calculates bed load and suspended load separately after splitting the total load. The sediment transport is calculated from the shear stress which is acting on the surface of the dunes.

It provides the results for (i) Sediment transport (ii) Accumulated erosion/sedimentation (iii) Bed load (iv) Suspended load (v) Dune height (vi) Dune length (vii) Manning's Roughness.

(4) The Van Rijn equation

The Van Rijn transport equation (Rijn, 1984) is based on relative magnitudes of bed shear velocity and particle fall velocity. Here the sediment load is calculated as bed load and suspended load separately. It requires the bed material sizes of D_{50} , D_{16} , D_{84} and D_{90} . The results are in the form of (i) Sediment transport (ii) Accumulated erosion/sedimentation (iii) Bed load and (iv) Suspended load.

3.3. Methods of simulation

In addition to the four different sediment transport formulae, there are two ways of computing the sediment transport rate in the morphological module. These are discussed as follows :

3.3.1. The explicit sediment transport models

The sediment transport computation are based on the results of the hydrodynamic computation using characteristic transport parameters. The sediment transport is calculated in time and space as an explicit function of the corresponding values of the hydrodynamic parameter i.e. discharge, water level etc.

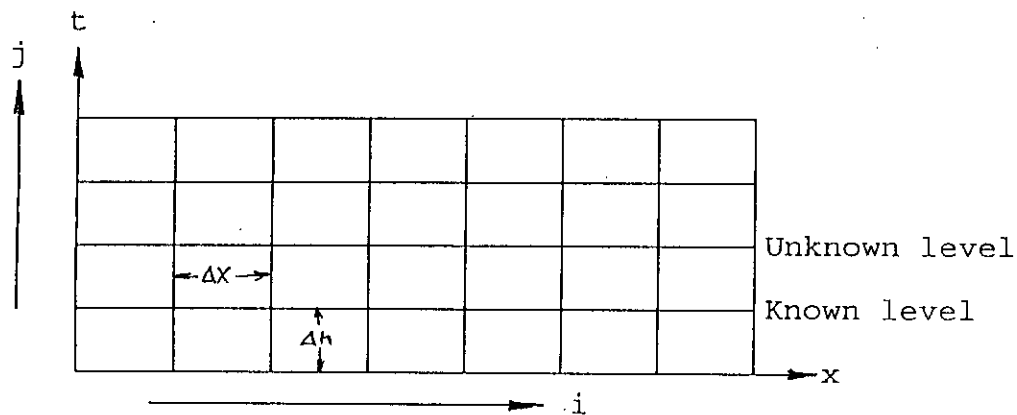


Figure 3.1 Representation of an explicit scheme.

Refer to figure 3.1 and consider a parabolic equation in the x-t plane as follows:

$$\frac{\partial \phi}{\partial t} = \frac{\partial^2 \phi}{\partial x^2} \quad (3.6)$$

Representing equation 3.6 into finite difference scheme in both time and space grid where i and j denotes the successive space and time increment according to the figure, we have

$$\frac{\phi_{i,j+1} - \phi_{i,j}}{k} = \frac{\phi_{i-1,j} - 2\phi_{i,j} + \phi_{i+1,j}}{h^2} \quad (3.7)$$

where h and k are space and time step respectively.

If we put $k/h^2 = r$, then the general form of an explicit formula can be written as:

$$\phi_{i,j+1} = r\phi_{i-1,j} + (1-2r)\phi_{i,j} + r\phi_{i+1,j} \quad (3.8)$$

This means that we have replaced $\frac{\partial^2 \phi}{\partial X^2}$ for the time step in going from j to $j+1$ by $[\partial^2 \phi / \partial X^2]_{i,j}$

From equation 3.8, it reveals that in an explicit formula there is only one unknown value which is a function of some known values.

Representation of an implicit formula:

From equation 3.8 it is evident that infinitively it would be better to use some average of $[\partial^2 \phi / \partial X^2]_{i,j}$ and $[\partial^2 \phi / \partial X^2]_{i,j+1}$

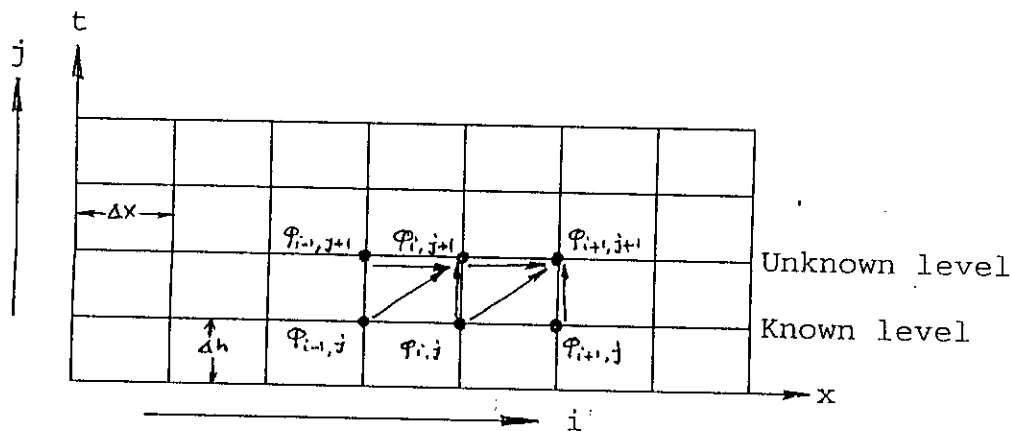


Figure 3.2 Representation of an implicit scheme.

The general weighted average formula can be written as:

$$AV = (1-\theta) \frac{\partial^2 \phi}{\partial x^2} + \theta \frac{(\partial^2 \phi)}{\partial x^2} \quad (3.9)$$

where, $0 \leq \theta \leq 1$

For $\theta = 0$, equation 3.9 represents an explicit formula.

when $0 \leq \theta \leq 1$, then equation 3.9 can be written as:

$$\begin{aligned} \frac{\phi_{i,j+1} - \phi_{i,j}}{K} = (1-\theta) \left[\frac{\phi_{i-1,j} - 2\phi_{i,j} + \phi_{i+1,j}}{h^2} \right] \\ + \frac{\theta [\phi_{i-1,j+1} - 2\phi_{i,j+1} + \phi_{i+1,j+1}]}{h^2} \end{aligned} \quad (3.10)$$

Taking $r = k/h^2$, we get

$$\begin{aligned} \phi_{i,j+1} - \phi_{i,j} = (1-\theta) r [\phi_{i-1,j} - 2\phi_{i,j} + \phi_{i+1,j}] \\ + \theta r [\phi_{i-1,j+1} - 2\phi_{i,j+1} + \phi_{i+1,j+1}] \end{aligned} \quad (3.11)$$

Segregating same time levels, we have

$$\begin{aligned} \phi_{i,j+1} - \theta r [\phi_{i-1,j+1} - 2\phi_{i,j+1} + \phi_{i+1,j+1}] = \phi_{i,j} \\ + (1-\theta) r [\phi_{i-1,j} - 2\phi_{i,j} + \phi_{i+1,j}] \end{aligned} \quad (3.12)$$

From this, the general form of an implicit equation can be written as:

$$\begin{aligned} -(\theta r) \phi_{i-1,j+1} + (1+2\theta r) \phi_{i,j+1} - (\theta r) \phi_{i+1,j+1} = (1-\theta) r \phi_{i-1,j} \\ + (1-2r(1-\theta)) \phi_{i,j} + (1-\theta) r \phi_{i+1,j} \end{aligned} \quad (3.13)$$

If $\theta = 0.5$, then the scheme is known as the Crank Nicholson implicit scheme as it was proposed by them.

3.3.2. The morphological model

'Morphology' means "the shape of"; thus river morphology concerns the shape of river and their channels. Channel morphology is the result of the interaction between the flow of water and sediment in the channel. A flow which is capable of transporting the alluvial material which forms its boundaries, both governs the hydraulic resistance i.e. there is a continual feedback between the sediment transport and the hydrodynamics.

A one dimensional morphological model is a model within which the hydrodynamic computation and the sediment transport computations are carried out in parallel. The bed level and the resistance numbers are updated in time and space as an explicit function of the corresponding value of hydrodynamic parameters, i.e. discharge, water level etc. Hence, changes due to the sediment transport is included in the hydrodynamic computation. Thus sediment transport phenomenon is modelled with continual feedback and therefore bed level changes can take place on the basis of a fixed bed hydrodynamic simulation. The model requires sediment/bottom level boundary conditions at inflow boundaries.

This work deals with the use of morphological model with sediment boundaries as a time series in the upstream boundary to simulate the bed level changes of the river

Ganges. Abbott's implicit scheme was used to solve sediment balance equations while computing in the MIKE11.

3.4 Flow resistance relationship

Dunes are the bed configuration which have the most important features for flow resistance because a dune in itself acts as roughness element. Where the bed is covered by bed forms, the total bed shear stress, τ , can be divided into two parts, τ' and τ'' . τ' is the shear stress acting on the gently curved upstream surface of the dunes, and τ'' is caused by the form drag on the dunes due to the fact that the water pressure is larger at the rear side than at the lee side.

Engelund (1966) found, by applying the principle of similarity, that a relationship exists between the dimensionless total bed shear stress, θ , and the dimensionless skin friction, θ' , which is described in Figure 3.3 .

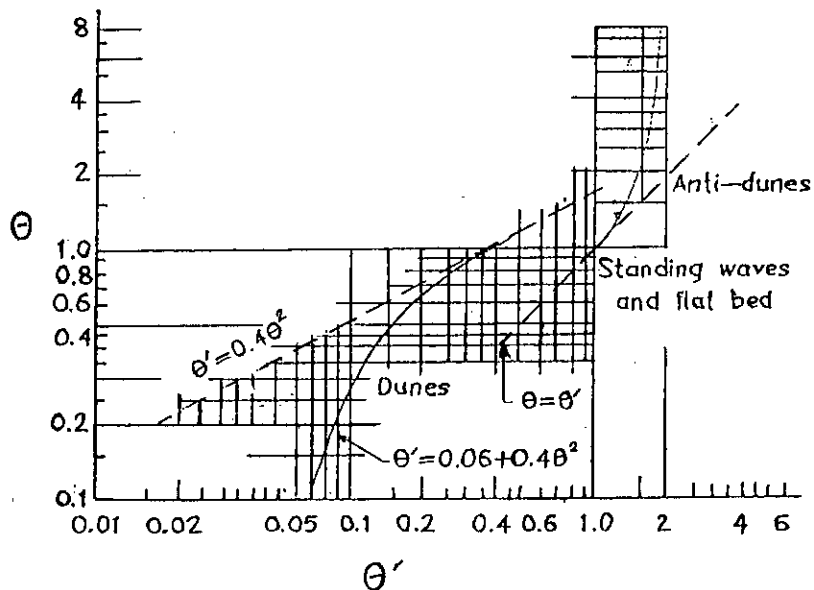


Figure 3.3 Plot of θ vs θ' (experimental data of different forms of waves), after Engelund (1966)

The relationship for a dune covered bed can be approximated by

$$\theta' = 0.4\theta^2 + 0.06 \quad (3.14)$$

where,

$$\theta = \frac{\tau/\rho}{(s-1)gd}, \quad \theta' = \frac{\tau'/\rho}{(s-1)gd} \quad (3.15)$$

ρ is the density of water, s is the relative density of the bed material, d is the mean grain size of the bed material and g is the acceleration of gravity.

In the case of a plane bed, the form drag becomes zero and the relationship reads:

$$\theta' = \theta$$

The relationship given in Equation 3.5 has been determined from flume observations. However, due to discontinuities in natural rating curves where two water levels may exist for a single discharge, these are two possible solutions to Equation 3.13 rendering it unsuitable for computer modelling. To overcome this problem, Challet and Cunge (1980) proposed a modified θ - θ' relationship as shown below. This is the formulation used in MIKE11.

$\theta \leq 0.06$	$\theta' = \theta$
$0.06 < \theta \leq 0.30$	$\theta' = 0.136\theta^{0.292}$
$0.30 < \theta \leq 0.90$	$\theta' = 0.06 + \theta^2$
$0.90 < \theta \leq 1.10$	$\theta' = 0.667\theta^{5.24}$
$1.10 < \theta$	$\theta' = \theta$

A detailed understanding of the flow over a dune-covered bed is obtained by the description of the figure below which is a vertical longitudinal section through the channel.

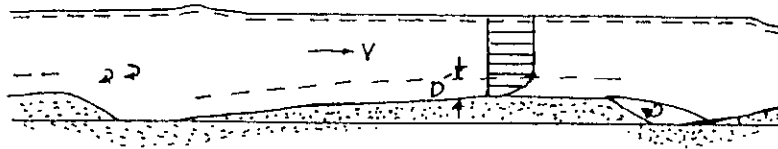


Figure 3.4. Flow over a dune covered bed.

Immediately downstream of the crest a large amount of turbulent energy is produced. This is dissipated into heat further downstream thus causing the expansion loss. At high Froude numbers a boil is formed at the water surface a little downstream from the expansion. At the end of the trough a boundary layer is formed, in which the velocity gradient is large, while the velocity distribution outside this layer is uniform.

The flow over the 'smooth' upstream side of the dune can be described by the boundary layer equation:

$$\frac{u}{u'_f} = 2.5 \left[\ln \left[\frac{30D'}{k} \right] - 1 \right] \quad (3.16)$$

u is the mean flow velocity, $u'_f = \tau'/\rho$, D' is the boundary layer thickness, $D' = D.\theta'/\theta$, D is the mean flow depth, and k is the equivalent sand roughness of the dune surface, $k \sim 2.5 d$.

Under weak non-uniform flow conditions, the steady state flow conditions can thus be found as a function of the specific discharge and the depth through the following four equations:

$$u'_f = \frac{u}{2.5 \left(\ln \left(\frac{30D'}{2.5d} \right) - 1 \right)} \quad (3.17)$$

$$\theta' = u'_f{}^2 / (s-1)gd \quad (3.18)$$

$$\theta = \sqrt{(\theta' - 0.06) / 0.4} \quad (3.19)$$

$$D' = D \cdot \theta' / \theta \quad (3.20)$$

Equations 3.17 to 3.20 can be solved by iteration.

The Manning coefficient can, if required, be calculated from the mean flow velocity, the depth and the total dimensionless bed shear stress, viz

$$\frac{g}{C^2} = \theta (s-1)gd \rho / u^2 \quad (3.21)$$

CHAPTER IV

SIMULATION OF BED LEVEL CHANGES

4.1 Introduction

The non-cohesive sediment transport module of MIKE11 is used for the simulation of bed level changes of the river Ganges by 1-D morphological modelling. The mathematical background and the inherent limitations of a one-dimensional mathematical modelling approach has already been discussed in chapter II and chapter III. The present one-dimensional modelling approach is based on the assumption that the width and alignment of the river remain unchanged during the simulation time. Prior to make input to the model, relevant data were collected and processed.

4.2 Data Collection and Processing

Following information regarding the simulation of the model have been collected and processed

1. Topographic data
2. Measured discharge
3. Observed water level
4. Observed sediment concentration
5. Gradation curves of bed material.

In the following sections detail descriptions of these data collection have been presented.

4.2.1 Topographic data

The principal objective of one-dimensional modelling is to carry out comparative runs to assess the potential impact of future changes to the rivers, such as the effect of confinement.

A total of 19 cross-sections in each year of the survey period 1988-89 and 1990-91 in the river Ganges have been collected and analysed. During simulation a channel is represented by smaller intervals for the following reasons:

- (a) To reduce the influence of an individual cross-section on water level, which is particularly relevant for the high degree of variability in cross-section.
- (b) To get a more accurate description of flood water profiles along the river reach.

Morphology division of BWDB surveyed the cross-sections of the Ganges river approximately at an interval of 6-7 km. along the river reach. Usually the Ganges river is surveyed almost every dry season at fixed locations along the same lines like other major rivers. The way by which MIKE 11 computes the sediment transport rates are affected by some factors which should be taken into careful consideration.

4.2.2 Discharge data

At Hardinge Bridge location (Station no. 60) discharge is measured regularly by BWDB. Most of the time the hydrology division of BWDB measured fortnightly discharge along with daily water level data. In this study observed discharges were taken for the period from 1985 to 1991. For the generation of the time series discharge boundary at Hardinge bridge from 1985 to 1991 the rating parameters given in Table 4.1 are used.

4.2.2.1 Discharge hydrograph of the Ganges

The comparison of the generated discharge hydrographs from 1985 to 1990 is shown in Figure 4.1. It is evident from the figure that in the monsoon season (Aug. to Sep.) the runoff is much higher in 1987 and 1988 from the average year 1986. Obviously, the increment of runoff in monsoon season concentrates mainly during flood period. According to the above mentioned figure peak discharge at Hardinge Bridge station in 1987 and 1988 were near about 75000 and 72000 m³/s respectively. When such kind of large floods synchronized with the floods in the river Jamuna, the fluvial process is affected on a large scale.

4.2.3 Water level

According to the BWDB regular water level measurement stations in the region concerned are listed below:

River	Location	Gauge no.
Ganges	Hardinge Bridge	90.0
	Sengram	91.1
	Mohendrapur	91.2
Padma	Baruria Transit	91.91
	Mawa	93.51

All these water level stations are used as comparison stations for the calibration of the hydrodynamic part of the model. For these all data were taken as a daily time series basis because there is no tidal influence in the study area.

4.2.4. Sediment data

The sediment data listed below in the form of both bed load and suspended load were collected and calculated as per BWDB schedule for the period from 1964 to onward (upto 1991-92).

River	Location	Gauge no.
Ganges	Hardinge Bridge	90.0
Padma	Mawa	93.51
	Baruria Transit	91.91

4.2.4.1 Analysis of sediment load

The amount of sediment load passing through a river system depends mainly on the relation of the sediment transport and the discharge, channel geometry, sediment control in the upstream, variations of the grain sizes etc. Due to the complex phenomenon of the discharge, sediment load and the channel geometry, the relationship between the sediment transport rate with discharge differs significantly from year to year or even in a particular year. To calibrate the sediment transport formula, observed sediment rating curve is developed by making a linear regression on a log-log plot of the observed sediment rate against observed discharge. The relations are shown in Figure 4.2 to 4.4 for the period of 1966-70, 1976-80 and 1966-89 respectively. It is revealed from the plots that there is a remarkable variations of the relation from year to year. Also there is significant difference between the sediment rating curve for the period 1966-70 and other curves after 1976. From Figure 4.2 it is observed that the rating curve for 1966-70 is more reasonable. Therefore, this rating curve is used for generating the time series sediment boundary as an inflow boundary to the model.

Again in order to study the reliability of the sediment rating curve, regression analysis was performed for the transport rate of measured load and discharge. The resulted correlation coefficients are given in Table 4.2. The average coefficient for the period of 1966-70 is 0.894, which indicates that the interpolated data of sediment discharge can be used with reasonable degree of accuracy.

The generated sediment discharge at Hardinge Bridge from 1985 to 1991 and that for water discharge which were used for both the time series boundaries in the model are shown in Figure 4.5.

4.2.4.2 Selection of representative grain size : Gradation curves analysis

To describe the representative grain sizes in the model, available gradation curves of bed material in the river Ganges is collected from RRI. From these curves it is observed that there is a large seasonal variation and also variation of transport rate even in a single cross-section. According to the availability of number of samples specially in the monsoon season, there is a paucity of sufficient data to establish a single set of grain sizes which will be the representative for the transport of sediment in the river. In most of the time, BWDB carried out sampling from the two banks and not from the bed of main conveyance channel i.e. from the maximum depth of flow. Hence, the large variation observed in the field data imposed a limitation to apply the van Rijn model for computing the bed level variation, because the van Rijn equation requires various sizes of bed material i.e. D_{16} , D_{50} , D_{84} and D_{90} . Due to non-availability of various grain dimensions the most simplest model which is formulated by Engelund-Hensen is taken for computation.

4.3 Sediment transport model set up

To simulate the bed level changes of the Ganges river, one dimensional model set up is applied. To avoid the effects of sediment boundary in the bottom level, the Ganges

river is extended about 100 km upstream. The river is also further extended downstream in the Padma river upto Satnal to make the model become unaffected from the boundary conditions. The schematization of the river in the model is taken after the analysis of the river cross-section data for the period 1988-89 and 1990-91.

4.3.1 Basis for schematization

This article gives an emphasis for the setting up of a simplified morphological model in the Ganges river. The influence of geometry of the channel which were used in the schematization of the river system was also emphasized. From the morphological point of view much of analysis is performed in the cross-sections of the river Ganges. It appears from the cross-section data that large bed level fluctuations have taken place at the Hardinge Bridge station at the high floods. This schematization was done by a smoothed section at the Ganges throughout the river reach.

The conveyance channels of a large river can be characterised by the presence of bed forms which propagate downstream during monsoon period. These bed forms in the Ganges can be identified as dunes and sand waves, the crest of which are irregular in plan. There is a wide variation of cross-sectional shapes occurred due to this large bed forms. The measured cross-sections at dry season which is 6-7 km apart is not good enough for the better resolution of shorter wave length of bed forms. According to the actual cross-sections in the Ganges river, there is a wide range of variation in the channel conveyance and therefore the sediment transport capacity. In practice, the conveyance and the sediment transport capacity at any given section will oscillate

between these limits during the year and from year to year.

Moreover, the rating curve at any location depends on the properties of the whole reach of the river. Therefore production of proper and correct rating curves, and storage at all points in a river system is utmost important from hydrodynamic point of view. This means that the variability of the conveyance in the measured cross-sections of the channel reach should be taken out by eliminating disturbance from the actual cross sections. Thus it is necessary to smoothen out this local variation of the conveyance before applying measured cross-section in the HD model. However, it should be noted that the length of the river is 117 km (app.) which is represented by 19 cross-sections as measured by BWDB, is not representative of the average properties of the river. In this study only cross-sections of 1988-89 and 1989-90 are analysed in order to smoothing out the variation of conveyance.

The computations in the present model are carried out on the basis of processed data of each cross-section containing the values of the conveyance area, hydraulic radius, storage width, additional storage areas and the resistance factors in the different levels of the section. The properties of these processed data were analysed to get indication about the channel properties which could be affected during the model run.

4.4 Conveyance analysis of the Ganges reach

The conveyance factor of the channel $AR^{2/3}$ and the hydraulic conveyance $MAR^{2/3}$, the two important factors of the channel, are to be analysed. The level dependent Manning number is taken by varying from one section to other by interpolating or adjusting the levels in the processed data of MIKE11. Hence conveyance factor is the most representative of the properties of the actual cross-section than the hydraulic conveyance. Figures 4.6 and 4.7 show the longitudinal profiles of constant conveyance factor along the Ganges reach. These profiles were drawn from the processed data of 19 cross-sections of 1988-89 and 1989-90. It reveals that when the conveyance factor is significantly low, then there is a remarkable variation from the mean channel gradient lines. At high conveyance factor the profiles are close to parallel. To analyse the properties of the cross sections, all properties were reduced to a an average datum. The water surface slope at bankfull discharge was considered to be the slope of the river Ganges. The bankfull conveyance profile corresponds to the bankfull stage was considered. A conveyance equals to $70,000 \text{ m}^{8/3}$ was taken as the bankfull conveyance for the Ganges river as a reference level for taking all levels into a common datum, so that at zero level all cross-sections will have the same conveyance (Figure 4.8). When all cross-sectional area were plotted against the reduced levels, it shows from Figure 4.9 that except for higher levels all conveyance area falls into one curve. In this way it can be possible to plot all 19 cross-sections in the same figure as shown in Figure 4.10.a to 4.10.f with the variation of conveyance factor, conveyance area, hydraulic radius, width, and Manning coefficient M respectively.

Similar procedure was followed for the analysis of 1989-90 cross-sections. All conveyance factors were reduced to a common datum and plotted together with the values from 1988-90 sections in Figure 4.11. It is seen that all conveyance factor falls into one defined shape. Hydraulic conveyance, area, hydraulic radius, width and model resistance number show little scatter at the higher levels. Thus, it can be concluded that Ganges cross-sections can be replaced by one single cross-sectional shape, and to be placed at appropriate levels and distance along the river reach.

There is insignificant difference from the bankfull conveyance profiles of 1988-89 after smoothing out of the profile, But this differences are not due to permanent bed level change. The mean difference is only 0.5 m at some locations at the Ganges.

4.5 Hydrodynamic schematization

By the development and propagation of dunes and sand waves in the river bed, the hydraulic conveyance and sediment transport capacity of each section fluctuates up and down about some mean level during the flood season. Due to local variation of cross-sectional area caused by bed undulation, there exists a large variation of local sediment transport rate. It is then utmost important to eliminate this noise and the sectional properties are then smoothed out in such a manner that average transport capacity of the river is unaffected. Thus the Ganges river has schematized with an identical cross-sectional shape which represents the average cross-sectional properties of the real section. The river is represented by its own equivalent cross-sectional

shape as shown in Figure 4.10.a. Through the river reach, the variation of the resistance factor with depth of flow is taken as uniform or constant. The hydraulic properties of the representative cross-section has shown in Figure 4.10.b to Figure 4.10.f.

To reduce the effect of sediment boundary to the bed and the simulated transport capacity of the inflow boundaries, the Ganges river is extended from Mathabhanga offtake to Pankha by 100 km. upstream and connected to the Padma river upto Satnal. For the river section at Padma the same methodology was carried out and same way was followed for schematization as stated in article 4.3.2. The scheme plan of the model setup is shown in Figure 4.12.

4.6 Boundary conditions

The model requires seven boundaries including both inflow and outflow boundaries as time series.

a) Inflow Boundaries:

- (1) Ganges extended: Discharge time series from Harding Bridge.
- (2) Ganges at 117 km.: Lateral Inflow boundary from Jamuna at Aricha.

b) Outflow Boundaries:

- (1) Padma at Shatnal: Water level time series.
- (2) Ganges at 49.5 km: Lateral outflow to Gorai as discharge time

series.

- (3) Padma at 60 km.: Lateral outflow to Upper Arial Khan as discharge time series.
- (4) Padma at 80 km.: Lateral outflow to Arial Khan as discharge time series.
- (5) Padma at 43 km.: Right bank spill from Padma, taken as lateral time series outflow.

All inflow and outflow boundaries were taken from April 1985 to October 1991. A simulation was carried out for the calibration of hydrodynamic model and transport formula. After calibration appropriate sediment rating curves were developed for the inflow sediment boundary. During the morphological computation the sediment rating curve is used as a time series sediment inflow at the boundary.

CHAPTER V

RESULTS AND DISCUSSIONS

5.1 Hydrodynamic calibration of the model

To check the water balance in the Ganges model Hydrodynamic performance test is carried out simultaneously with actual and idealized sections used in the model schematization. The simulation period is taken from April 1984 to October 1991. The results are shown in Figures 5.1 and 5.2. The comparison between simulated and measured water levels in the river Ganges are shown in Figure 5.1. From the figure it is observed that the calibration is quite satisfactory using the equivalent cross-sections in the Ganges both for low and high water levels. From the Figure 5.2 the discharge at Baruria is well matched in every year after combining the discharge from Jamuna. Water level at Baruria and Mawa were also matched reasonably except an average of 0.40 meter deviation observed at high flows in 1989 and 1990 in both the stations.

5.2 Sediment transport model

According to the fluvial process, the suspended load coarser than D_5 or D_{10} is called bed material load, whereas that finer than D_5 or D_{10} is wash load. In general, the channel deformation is caused by the exchanging process between the coarser suspended and bed material. In the Engelund-Hansen model a median size D_{50} of the bed material is used. Hence, during the flood season and in the main conveyance

channel it is observed that variation of the bed material of median size D_{50} exists. For the Padma river the sizes were taken from the gradation curves of bed material Meghna River Bank Protection Study (1992). The selected sizes are shown in Table 5.1 and the selection was performed by trial and error basis after obtaining near equilibrium of the transport rates (Figure 5.3).

5.3 Model run

To establish an equilibrium of sediment transport rate along the channel reach and for selecting the representative grain size in the model, 1st run was made taking no change in bed level in the sediment transport file. The model can run both explicitly as well as implicitly. In the implicit model run, updating of bed level takes place simultaneously after every hydrodynamic computation. So an implicit model run was carried out using the sediment time series in the upstream boundary. The computation was carried out using the Engelund-Hansen formula such a way that hydrodynamic computation was carried out after every four hours but sediment transport and bottom level updating was computed after every four days. The hydrodynamic and morphological results were saved after every four days.

5.3.1 Calibration of sediment transport model

The model is calibrated by the consideration of the following conditions:

- (a) The hydrodynamic performance of the model i.e. the hydrodynamic calibration (water level, discharge) is reasonably matched. This criteria was fulfilled as stated earlier in Figure 5.1 and Figure 5.2.

(b) Comparison of sediment transport rate, Figure 5.4 shows the comparison of computed transport rate with that of the observed values during the period of 1985 to 1991. The plot shows a reasonable agreement with the observed transport rates from year to year except for higher values in the flood year i.e. 1987 and 1988. In the two years, the model simulates the lower rates than those observed. In 1989 the overall trend is quite good but the model simulates some higher values but still it is in the allowable limit in comparison to the calibration of the sediment rates. Figure 5.4 reveals that both for high and low values the comparison is quite satisfactory for 1985, 1986, 1990 and 1991.

With the model results an equation relating the simulated transport rate with the observed transport rate was developed. Figure 5.5 shows a plot of computed transport rate vs observed transport rates. After regression a fitted curve was drawn showing the simulated and observed values. The fitted line show a very near to the 45° line. The equation is also presented in the same figure which corresponds to the modelled values.

5.3.2 Model results and analysis

From the model results the annual discharge and sediment load for the station Hardinge Bridge during the period 1985 to 1991 are given in Table 5.2. The average annual runoff in the last seven years is computed as 359×10^9 m³/s and for the same period the average annual sediment load at Hardinge Bridge is computed as 0.26×10^9 tons. From this result, the variation of annual discharge and and annual total load at

Hardinge Bridge is shown in figure 5.6.

The comparison between the results of this study after model computation and that of MPO (1987), FEC (CBJET,1991) and Coleman (1969) are given in Table 5.3.

From the table it can be concluded that on an average the computed annual sediment load is reasonable.

5.4 Distribution of runoff and sediment load

The distribution of the runoff and the sediment load for the station Hardinge Bridge are listed in Tables 5.4 and 5.5 during the period from 1985 to 1991. The runoff and sediment load are mainly concentrated in the monsoon season. The flow from July to September at Hardinge Bridge station for the period from 1985 to 1991 accounts for 70.65 percent of the total flow and the sediment load for the same period is 80.53 percent of the total.

5.5 The statistical parameter of the sediment load

The statistical parameters of the computed annual sediment load are listed in Table 5.6. It is observed that the standard deviation is quite low (0.0466) for the period from 1985 to 1991 and the annual maximum load occurred in 1987 to 1988 period amounts to 0.305×10^9 tons.

5.6 Bed level variation of the river Ganges

A net amount of aggradation and degradation in the river reach from 1985 to 1991 is shown in Figure 5.7. The amount is shown as volume of net erosion and deposition along the river reach.

From this figure it is observed that during this period the net amount of erosion at the upstream of Hardinge Bridge constriction (chainage 32.5 km) is about $12 \times 10^{10} \text{ m}^3$. After the constriction from km 52, deposition was experienced in the successive chainages upto 104 km. Among the chainage between km 52 and km 104, a maximum deposition observed at km 52 and km 71.5 (Location of Sengram) are about 12.5×10^{10} and $9 \times 10^{10} \text{ m}^3$ respectively.

Figure 4.20 shows the net annual variation of bed level from 1985 to 1991 for the locations at Hardinge Bridge (Km 32.5), Sengram (km 71.5) and Mohendrapur (km 97.5).

Table 4.1: Rating parameter at Hardinge Bridge.

Year	Interval-1			Limit1	Interval-2		
	a	b	c		a	b	c
1985	2.2	2.83	27.15	10.80	9.1	2.95	1991
1986	2.0	2.97	19.44	10.66	8.7	2.43	1821
1987	2.0	2.91	16.05	10.00	9.0	2.86	1622
1988	2.1	2.30	68.25	11.00	9.5	2.46	1763
1989	2.0	2.83	20.10	10.00	9.3	1.97	4240
1990	1.2	2.75	20.81	12.00	9.5	1.44	5511
1991	2.1	2.97	15.62	12.00	9.8	1.84	3031

Note: Equation of rating curve $Q = c(WL-a)^b$

where, a = Level at zero discharge.

c and b are constant and exponent respectively.

Limit1 = Upper limit of water level for interval-1.

Table 4.2: Correlation coefficient for the sediment transport rates and discharge.

Period	1966-70	1976-89	1966-89
Coefficient of correlation	0.89	0.65	0.72
Standard error of co-efficient	0.08	0.10	0.07

Table 5.1: Grain diameters used in the model.

River name	River Chainage (Km)	D ₅₀ (mm)
Ganges	0.0	0.17
Ganges	117.0	0.13
Padma	0.0	0.13
Padma	100.0	0.09
Ganges-extension	0	0.18

Table 5.2: Computed annual flow and annual sediment load for the station at Hardinge Bridge (1985-91).

Period	Annual flow (m ³ /s)	Annual sediment load (unit: 1*10 ⁸ tons)
1985-86	13003	2.94
1986-87	11160	2.41
1987-88	12248	3.05
1988-89	11548	2.83
1989-90	8648	1.57
1990-91	12526	2.78
1991-92	10604	2.75
Average in 7 years	11391	2.6
V	3590	

Note: V = average annual runoff in 7 years in 1*10⁸ m³.

Table 5.3: Comparison of the annual sediment load
(unit: 1×10^9 Ton)

River : Ganges.

Station : Hardinge Bridge.

MPO (1987)	0.212
FEC (CBJET,1991)	0.338
Coleman (1969)	0.478
CBJET (1991)	0.196
Present study	0.261

Table 5.4: Percentage of monthly runoff and sediment load
(1985-91).

River : Ganges.

Station : Hardinge Bridge.

Item	Apr	May	Jun	Jul	Aug	Sep	Oct	Nov	Dec	Jan	Feb	Mar
Runoff	.654	.969	2.77	14.59	29.25	26.79	12.91	4.24	1.97	1.27	.77	.628
Sediment Load	.133	.199	.785	12.85	33.68	33.99	11.58	2.08	1.41	.308	1.03	.128

Table 5.5: Distribution of runoff and sediment load from July to September.

River	Station	Period	Runoff.	Sediment load.
Ganges river	Hardinge Bridge	1985-91	70.65%	80.53%

Table 5.6: Statistical parameter of the computed annual sediment load (period 1985-1991).

Period:1985-91 Station:Hardinge Bridge	Average.	δ (Standard deviation)	Cv (Coefficient of variance)	Annual maximum Unit: 1×10^9 Ton	Annual Minimum Unit: 1×10^9 Ton
	0.261	0.0466	0.179	0.305(1987-88)	0.157(1989-90)

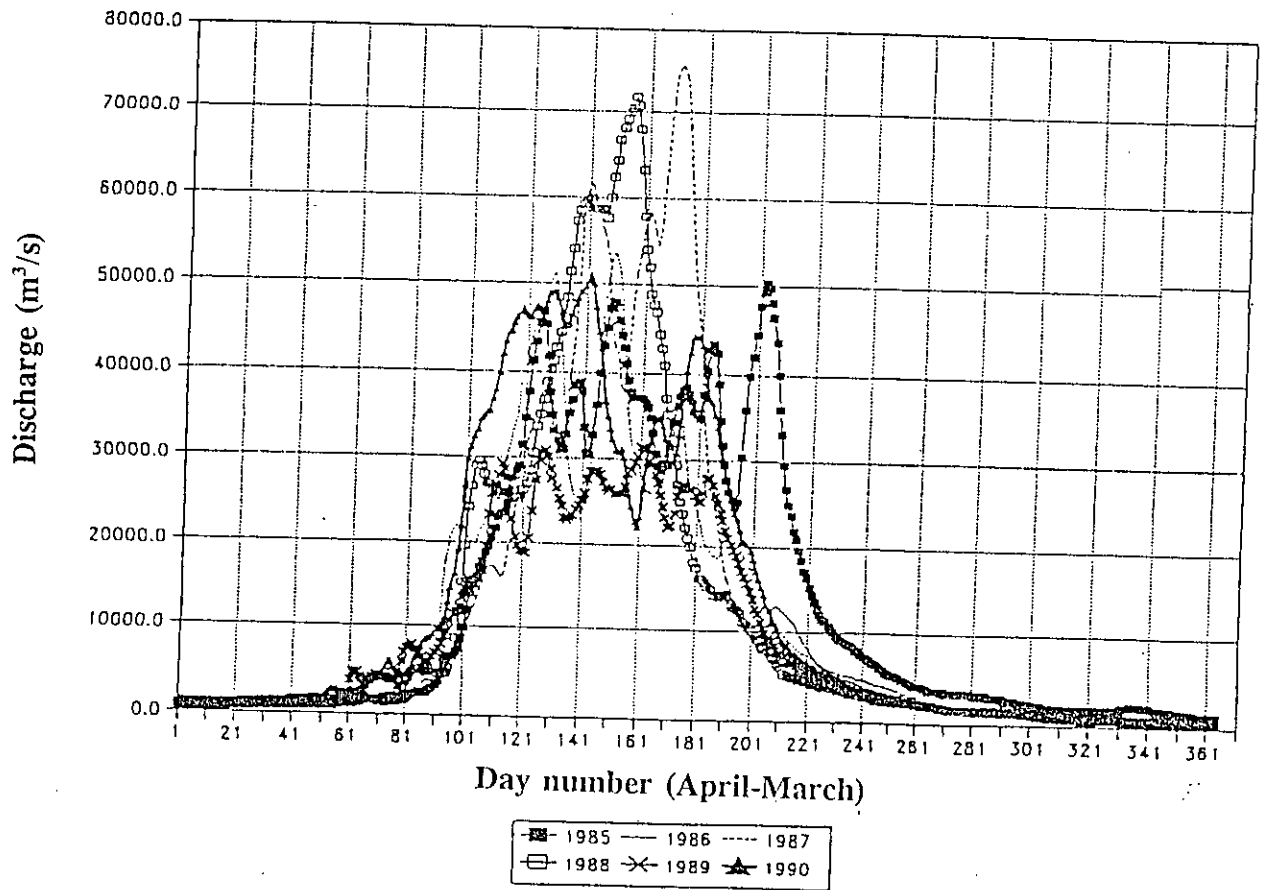


Figure 4.1 Comparison of the generated discharge hydrograph at Hardinge Bridge

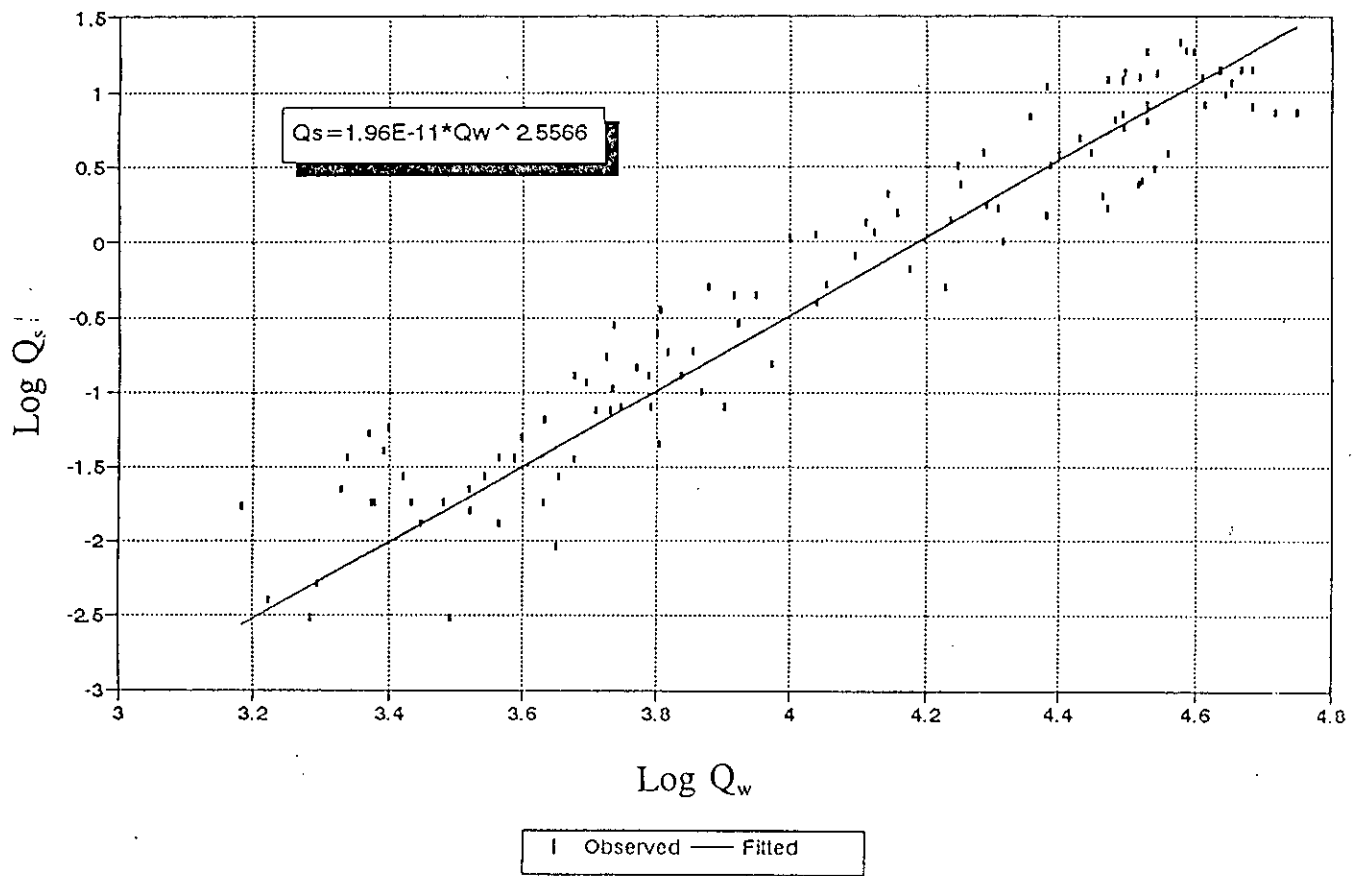


Figure 4.2 Sediment rating curve at Hardinge Bridge (1966-'70)

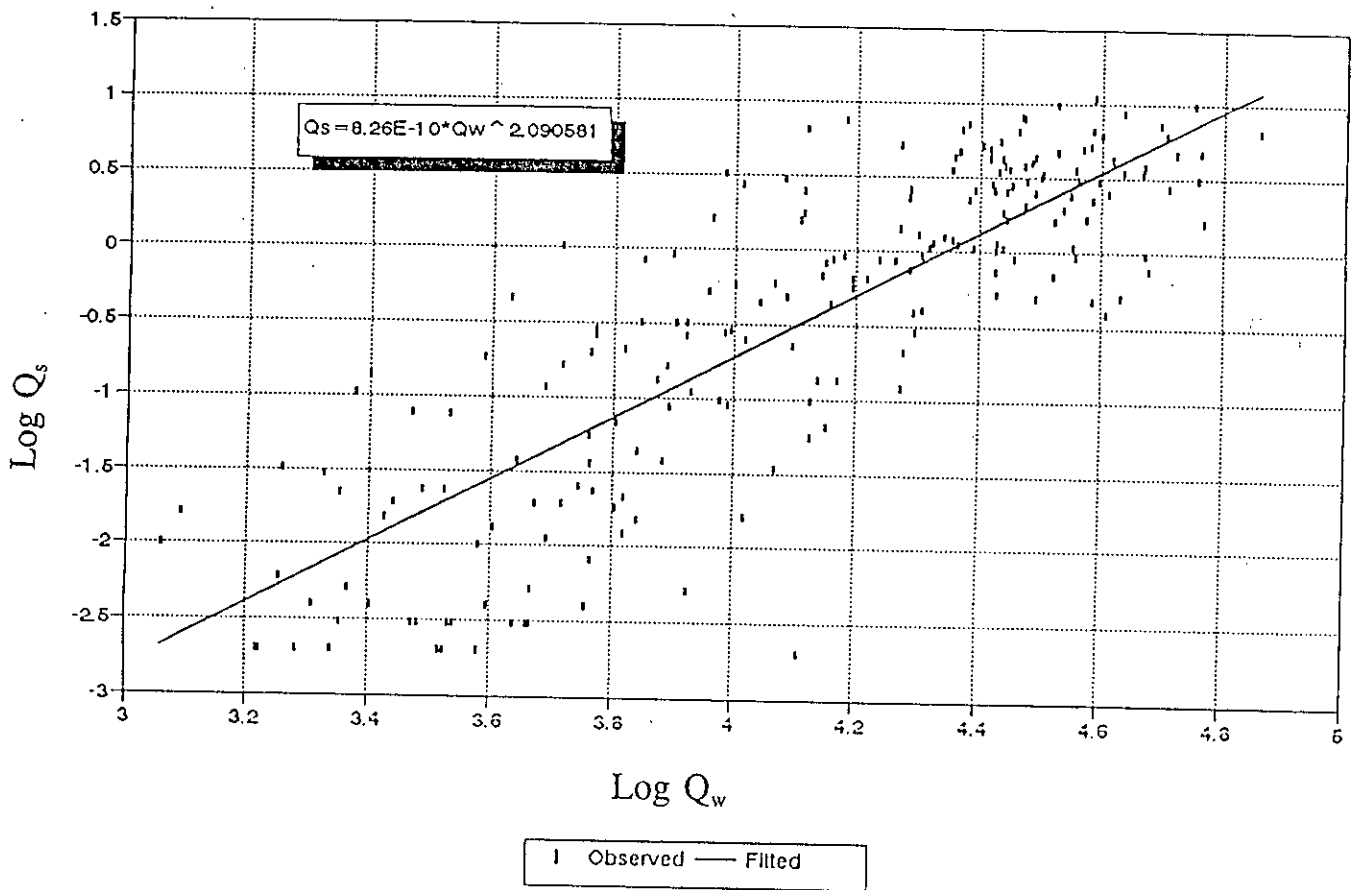


Figure 4.3 Sediment rating curve at Hardinge Bridge (1976-'89)

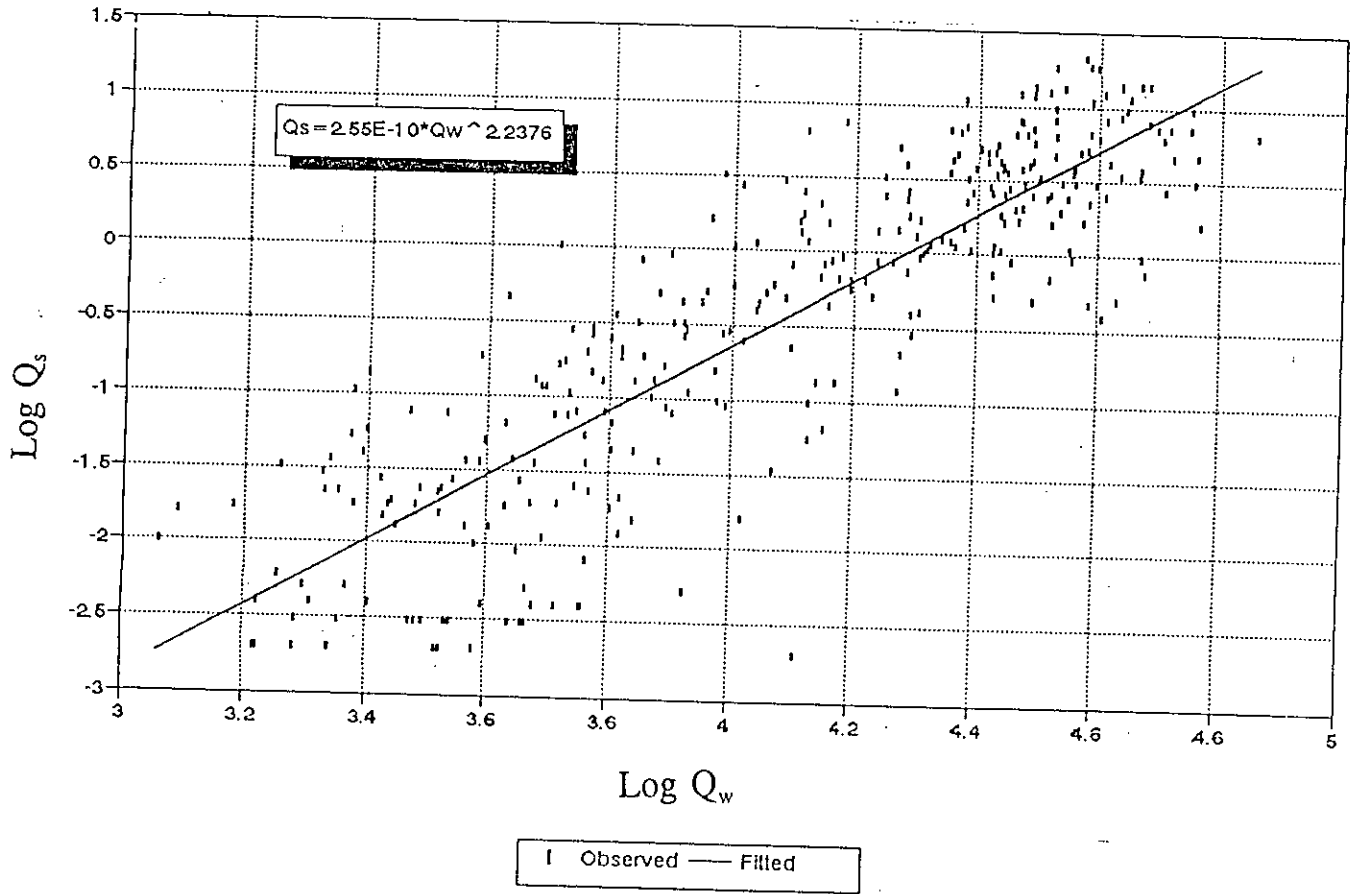


Figure 4.4 Sediment rating curve at Hardinge Bridge (1966-'89)

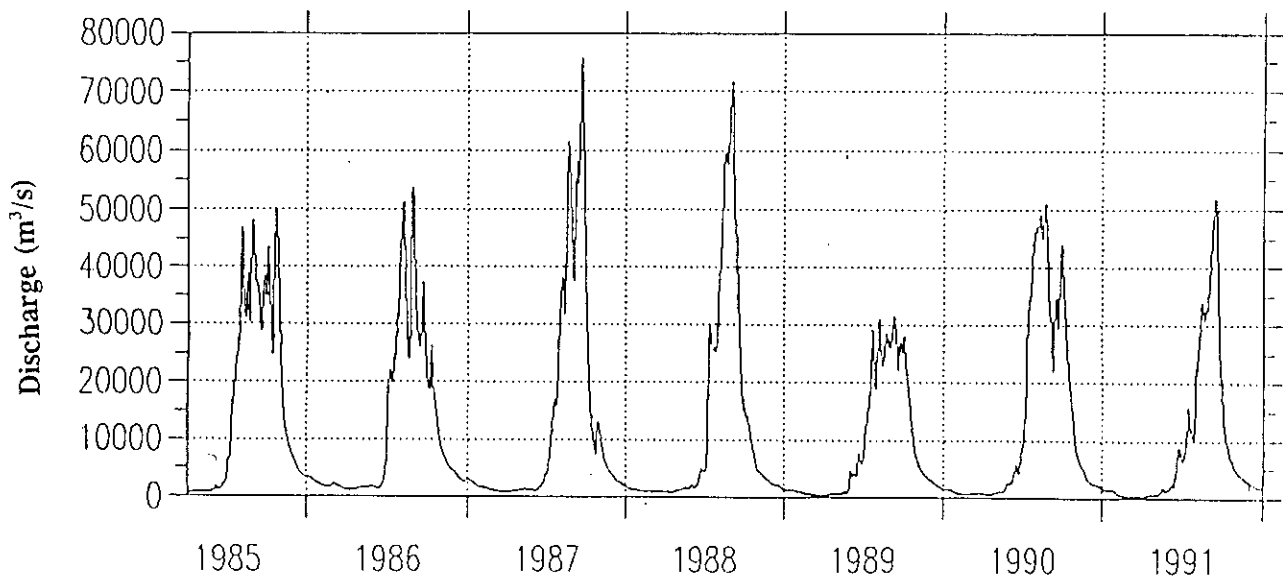
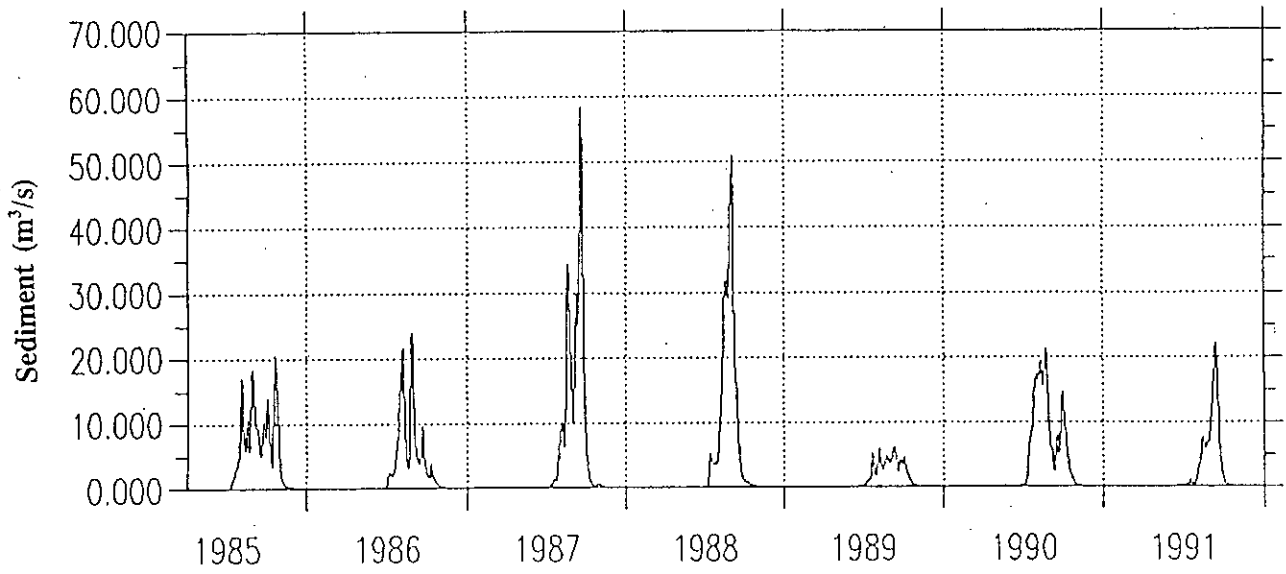


Figure 4.5 Generated sediment and discharge hydrograph at Hardinge Bridge

River : Ganges
 Surveyed : 1988-89
 $Y = -0.0569528X + 15.6459$

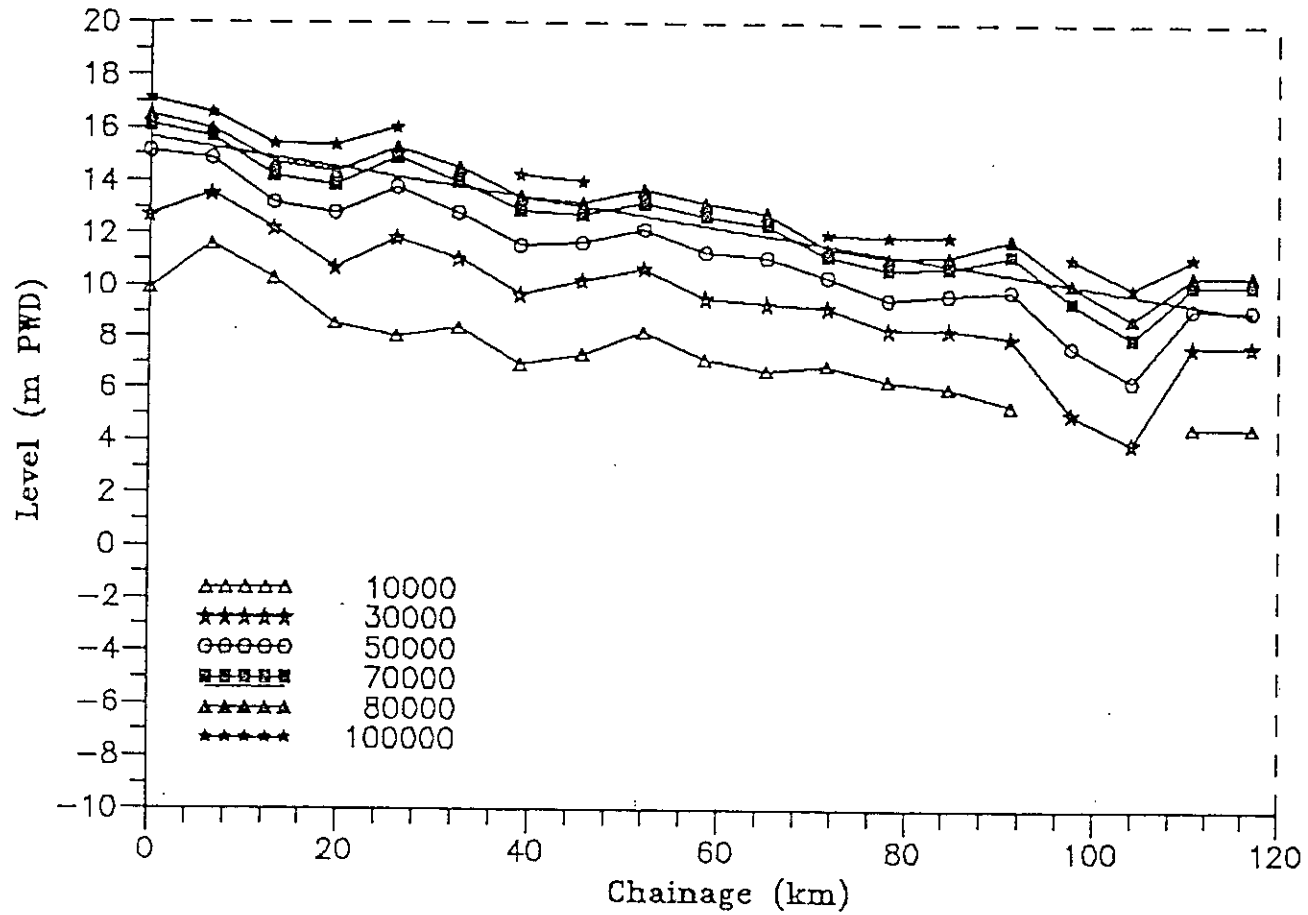


Figure 4.6 Equi conveyance profiles for the Ganges (1988-'89)

River : Ganges
 Surveyed : 1990-91
 $Y = -0.0487045X + 14.6229$

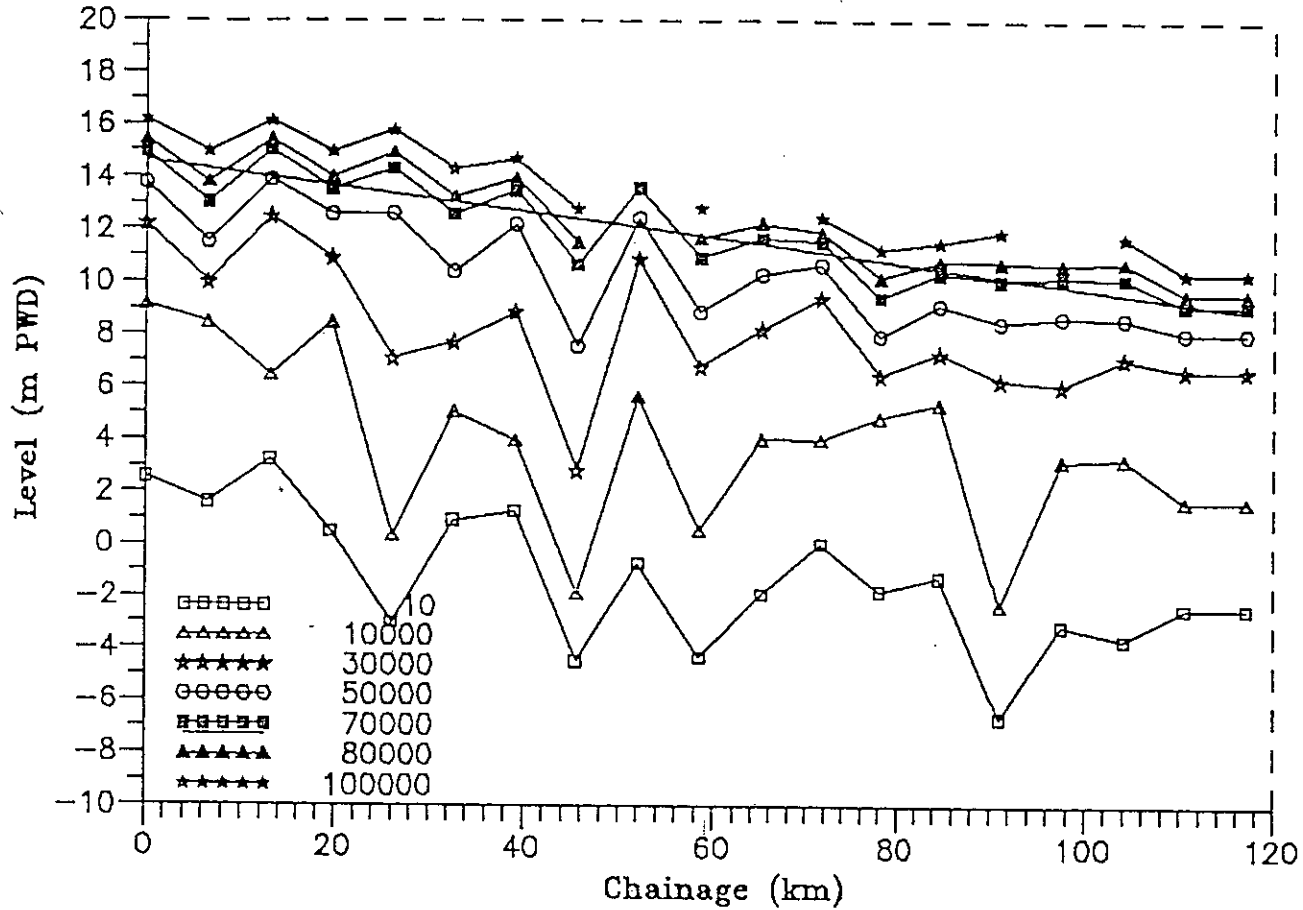


Figure 4.7 Equi conveyance profiles for the Ganges (1990-'91)

River : Ganges
Surveyed : 1988-89

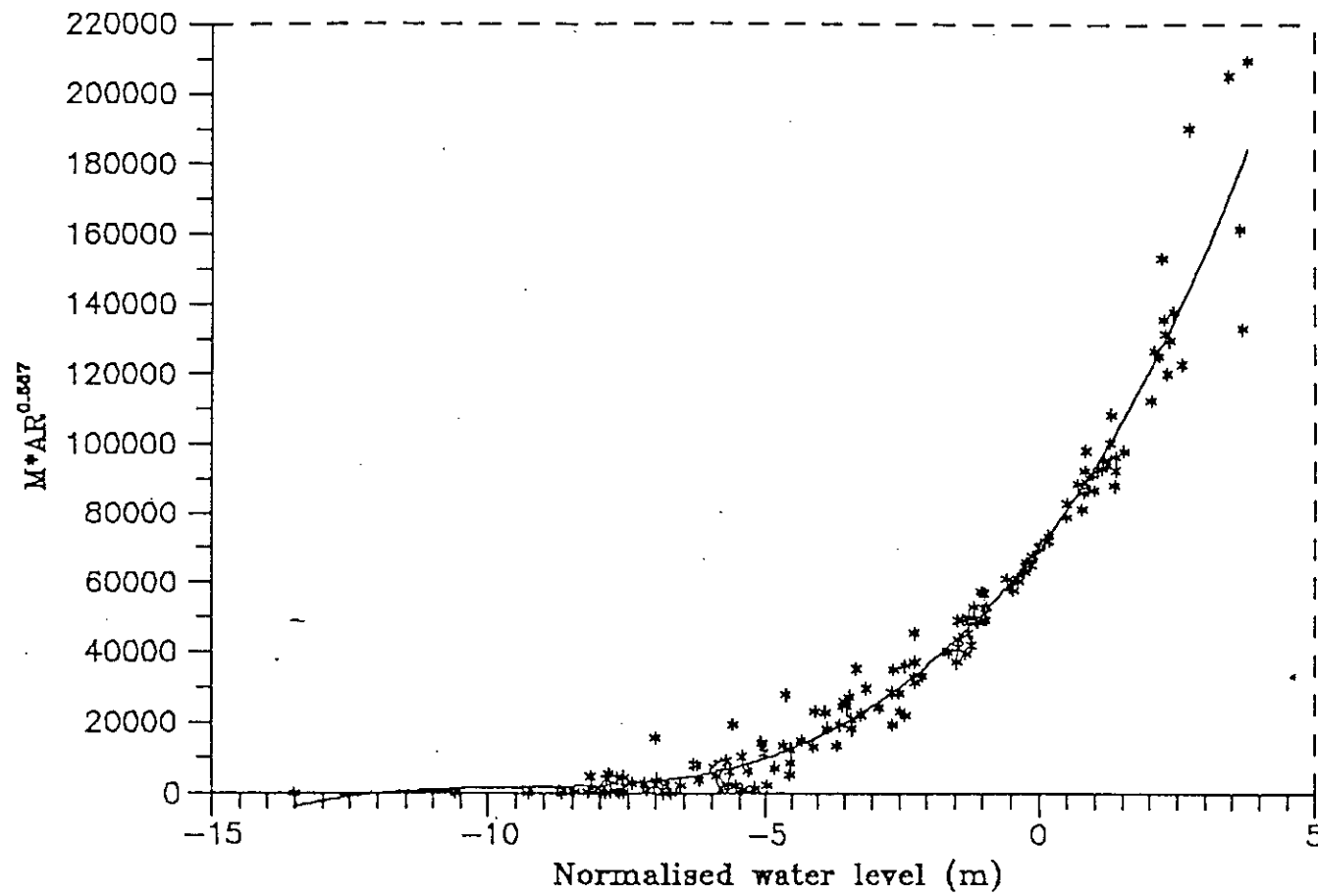


Figure 4.8 Model conveyance curve (1988-'89)

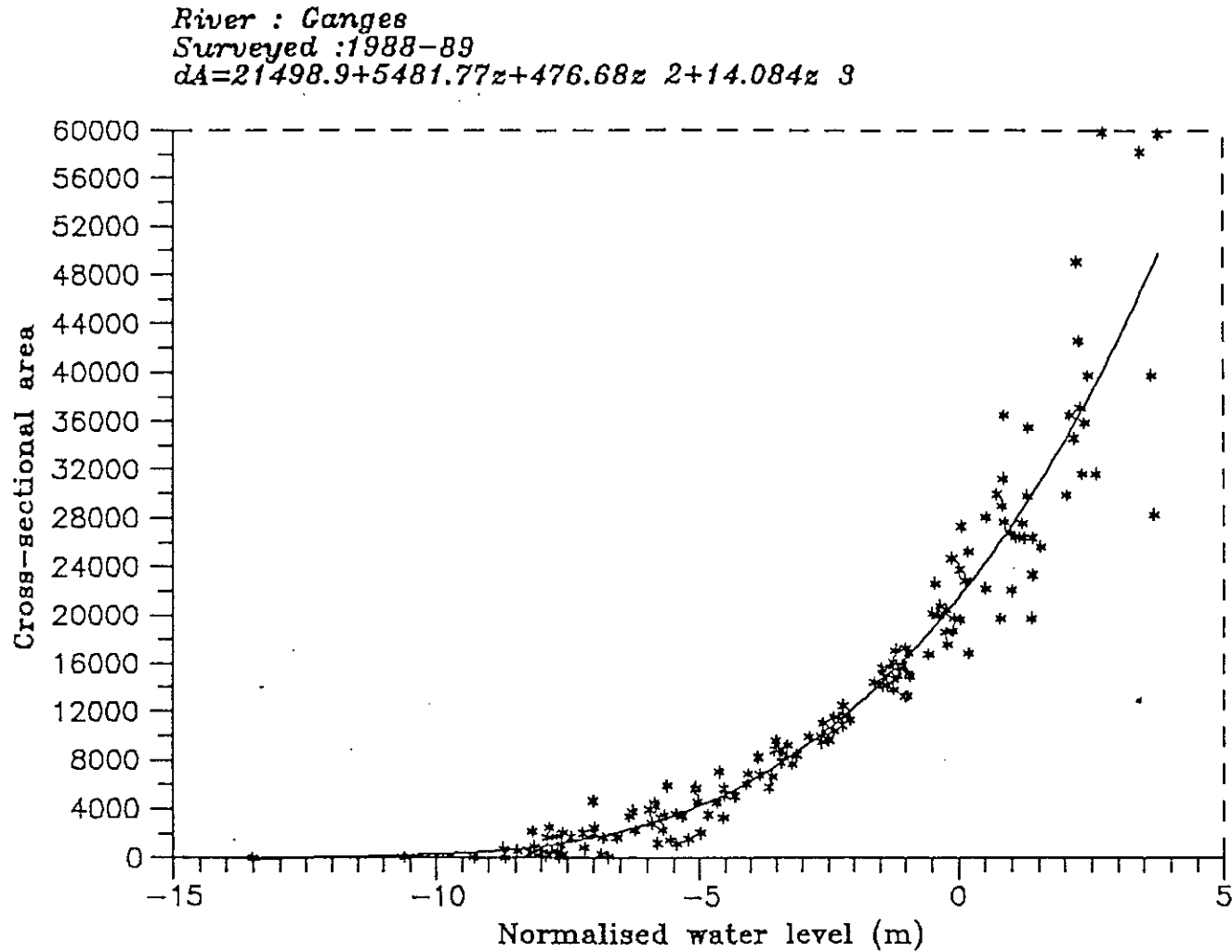


Figure 4.9 Cross-sectional area vs normalized waterlevel (1988-'89)

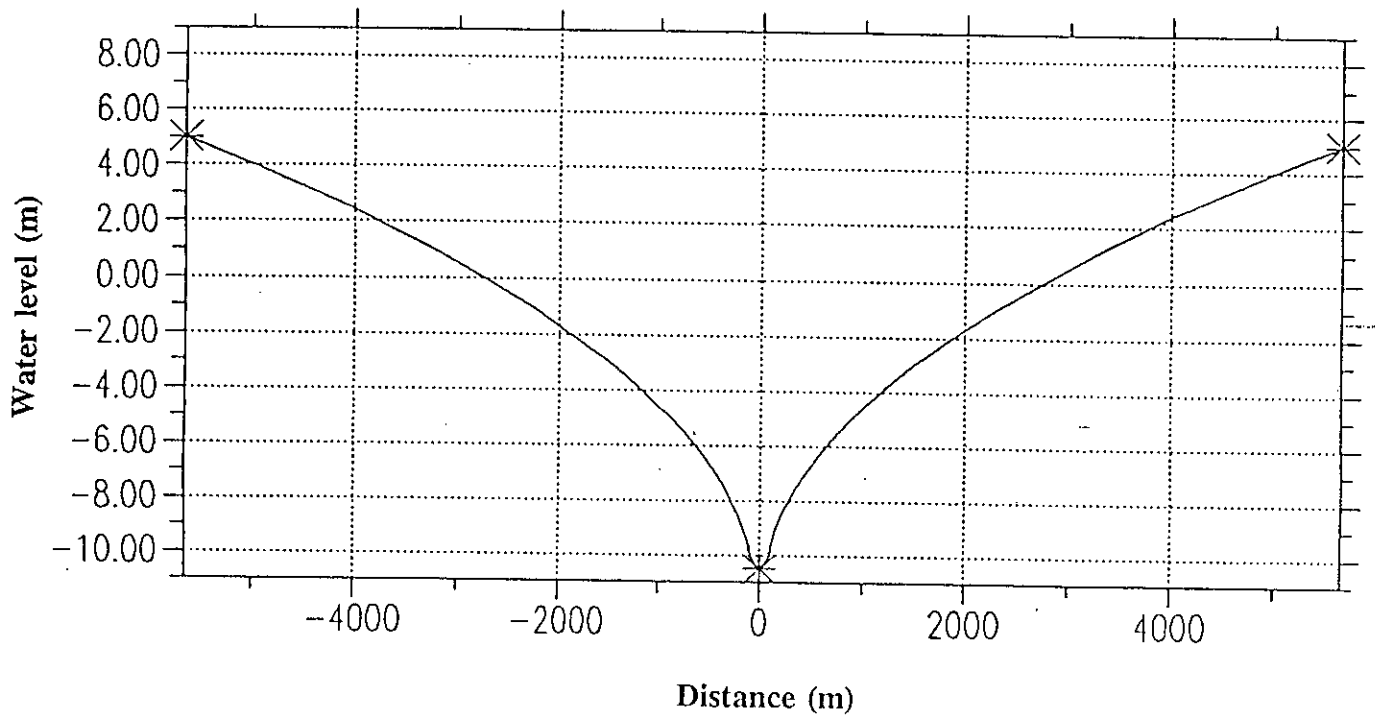


Figure 4.10.a Idealized cross-section of the river Ganges

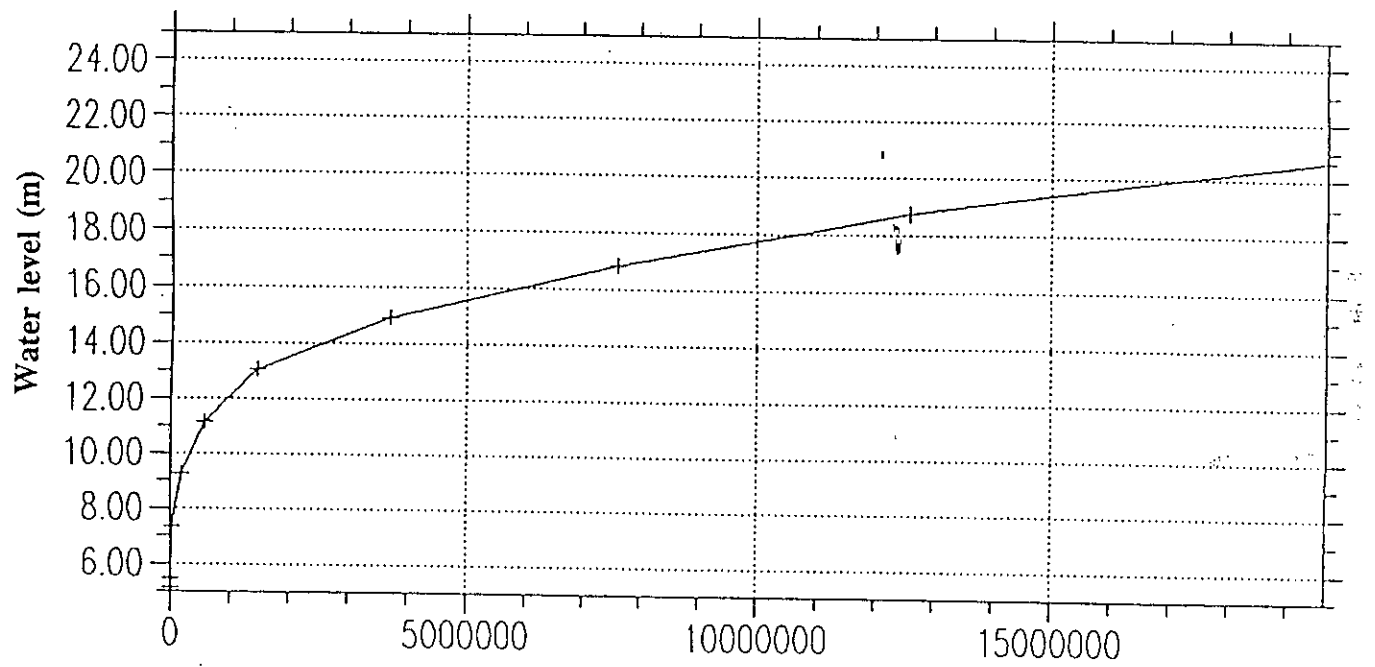


Figure 4.10.b Conveyance vs water level curve for idealized section

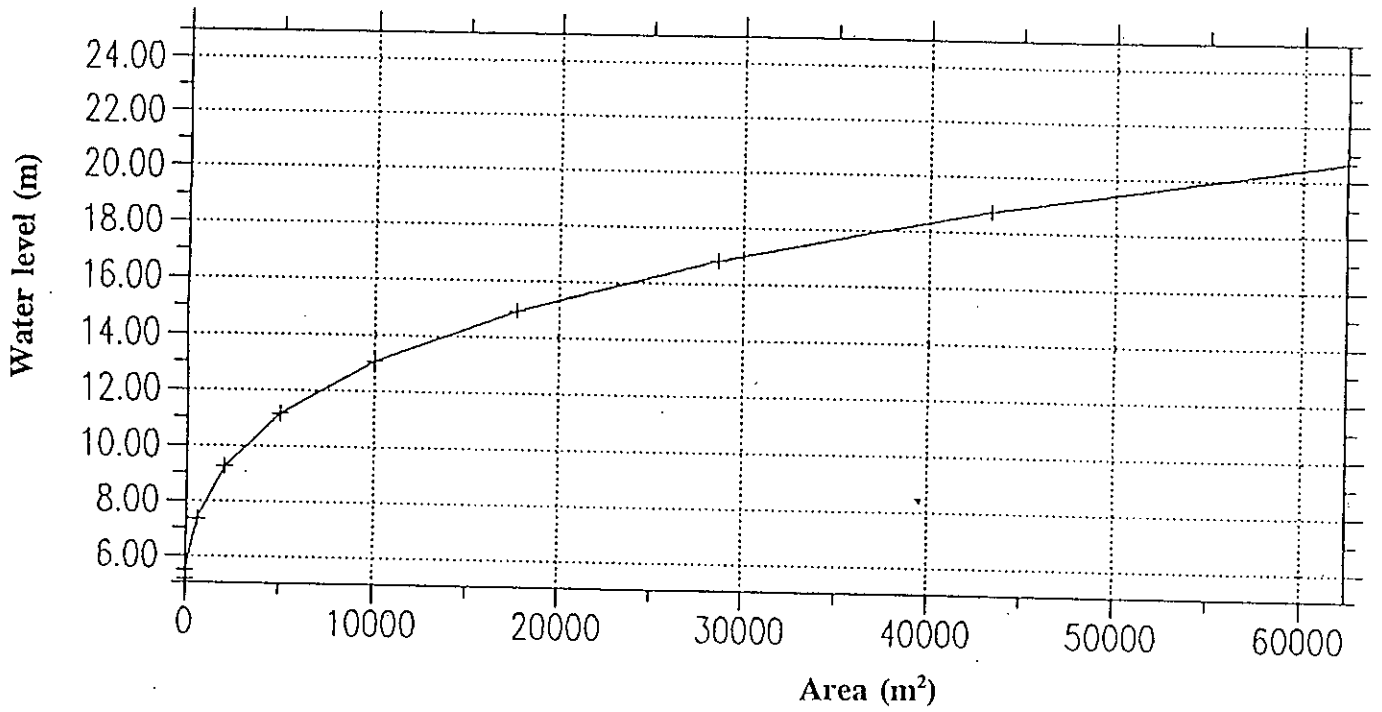


Figure 4.10.c Area vs water level curve of the idealized section

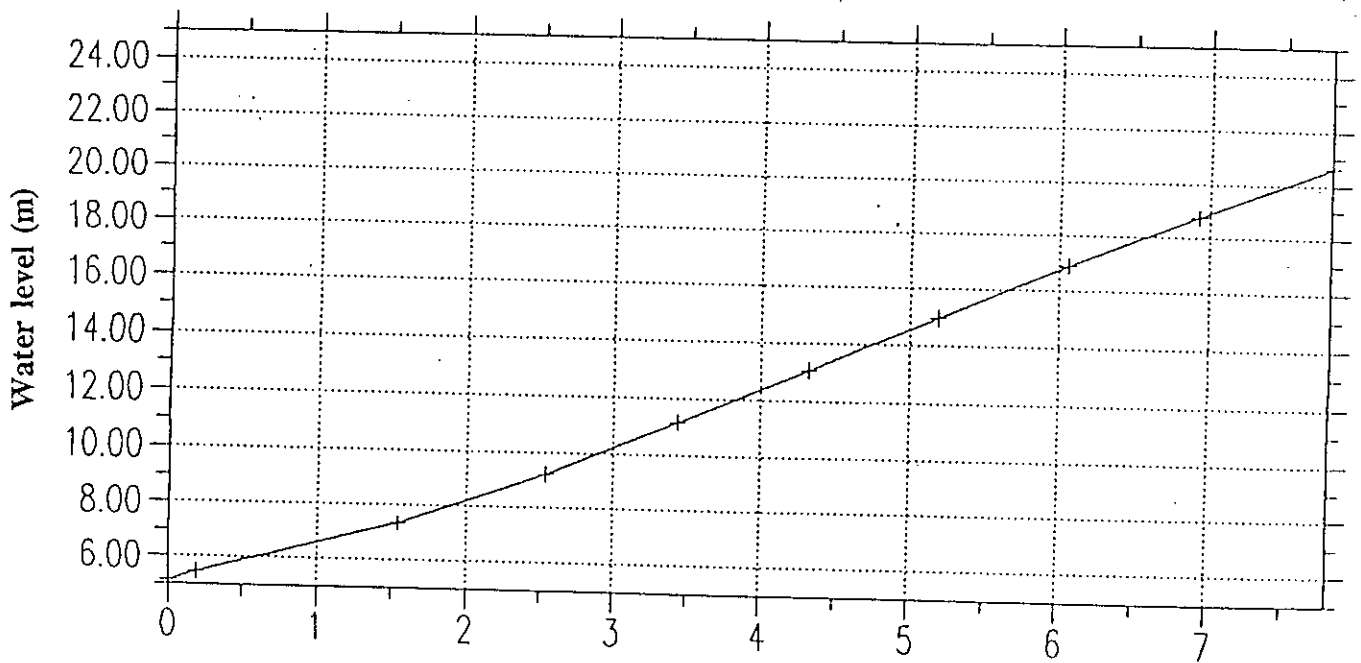


Figure 4.10.d Hydraulic radius vs water level curve of the idealized section

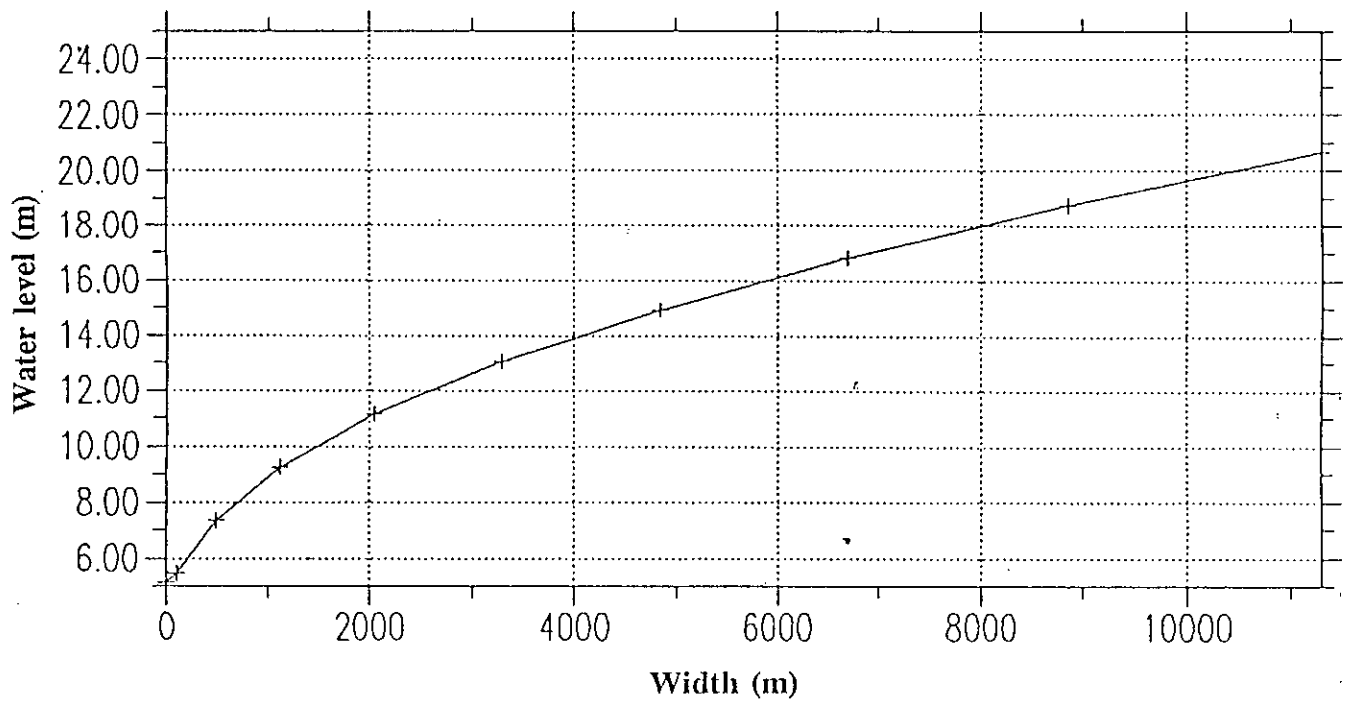


Figure 4.10.e Width vs water level curve of the idealized section

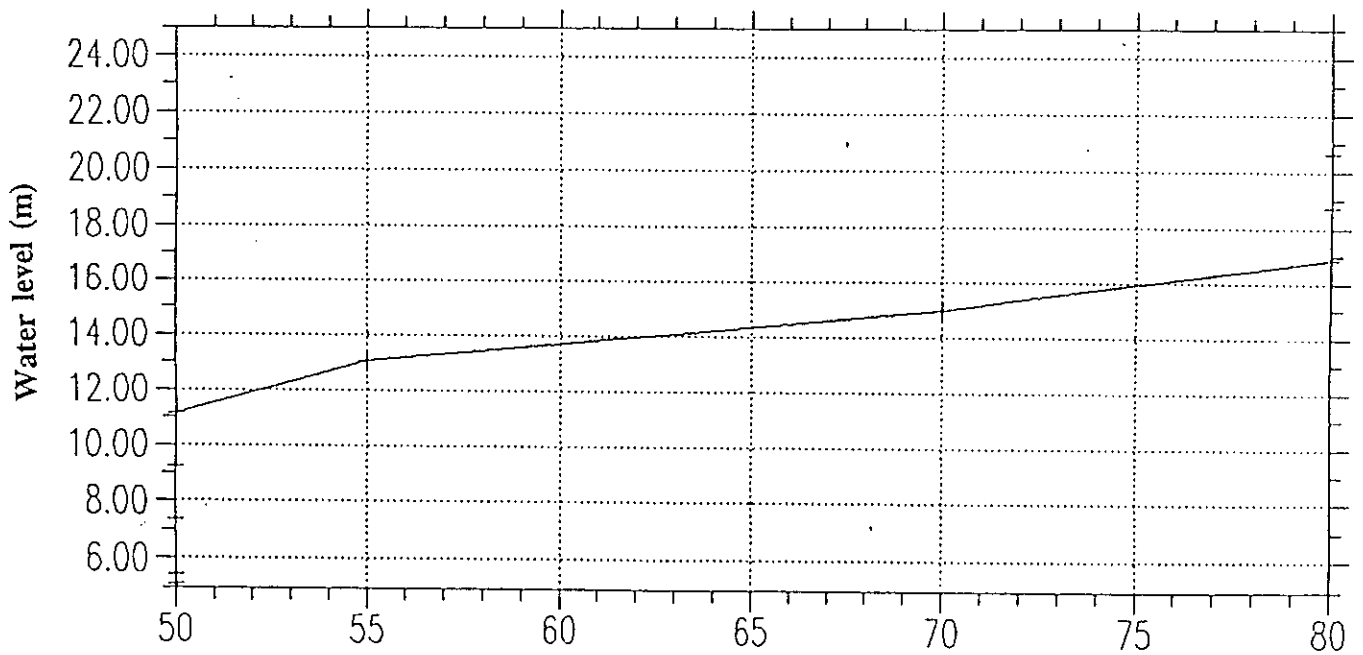


Figure 4.10.f Resistance factor vs water level of the idealized section

River : Ganges
 Surveyed : 1988-89 & 1990-91
 $Y = -0.0569528X + 15.6459$

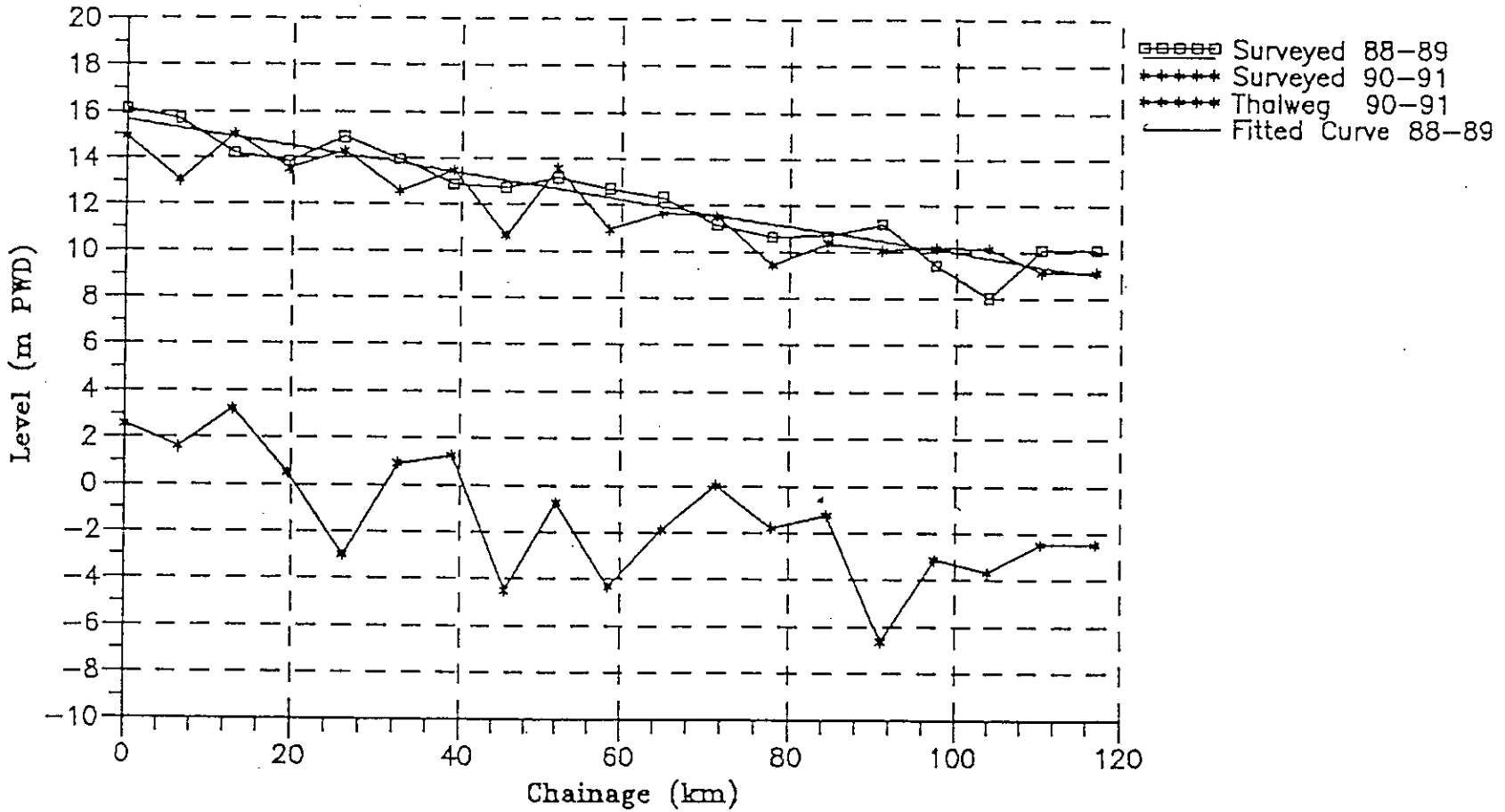


Figure 4.11 Equi conveyance profiles at bankfull conveyance (1988-'89 and 1990-'91) of the Ganges

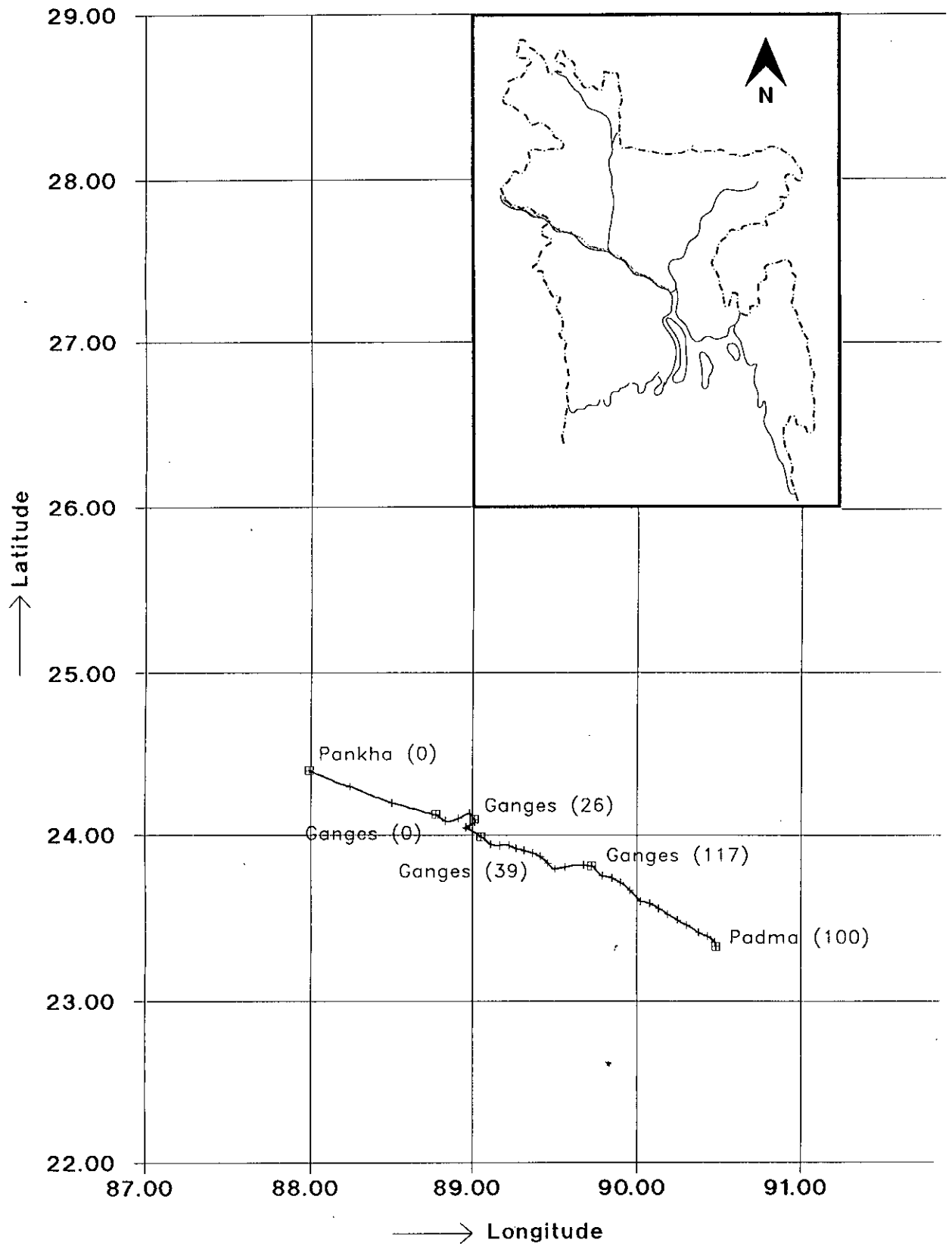
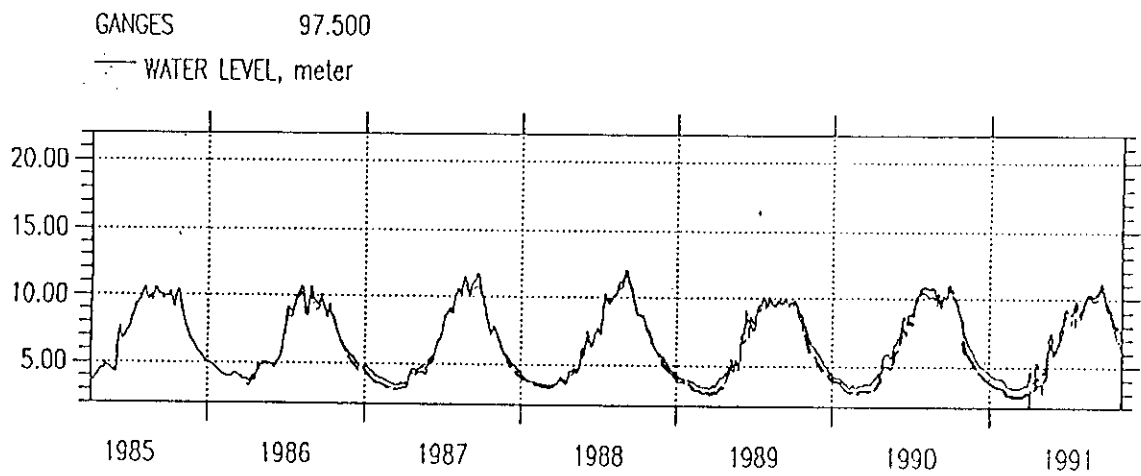
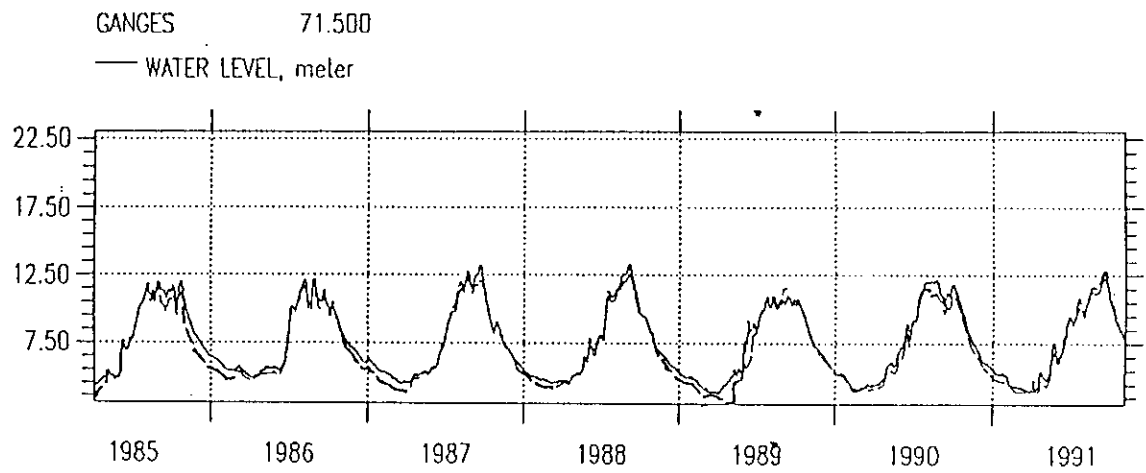
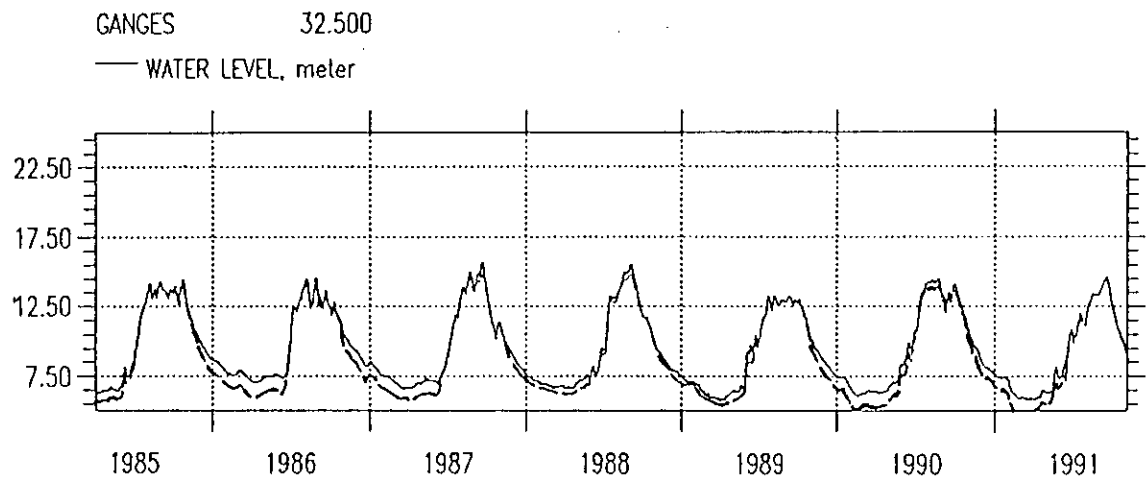


Figure 4.12 Scheme plan of the model



----- Observed ————— Simulated

Figure 5.1 Calibration of the hydrodynamic model at Hardinge Bridge, Sengram and Mohandrapur

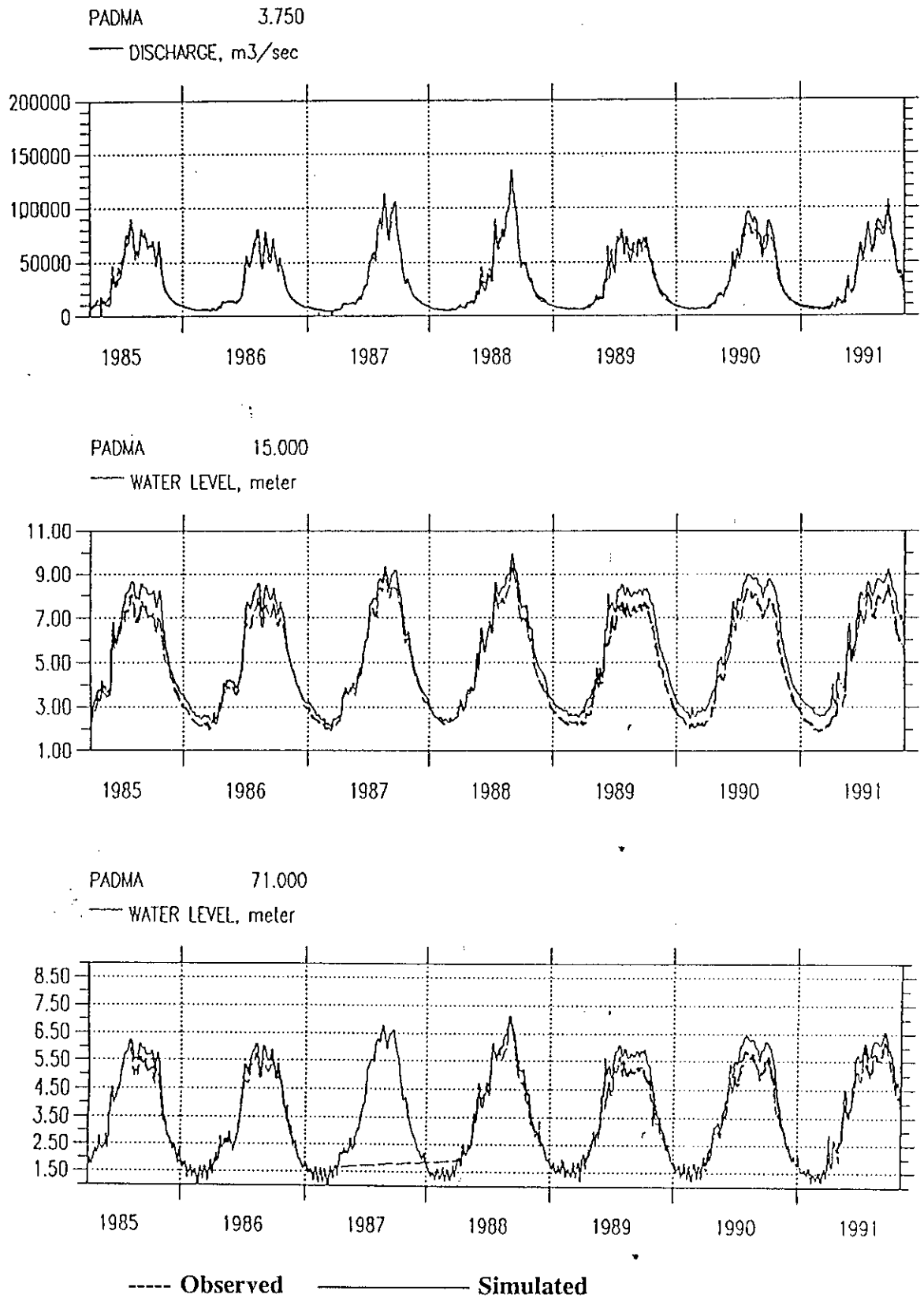


Figure 5.2 Calibration of the hydrodynamic model at Baruria and Mawa

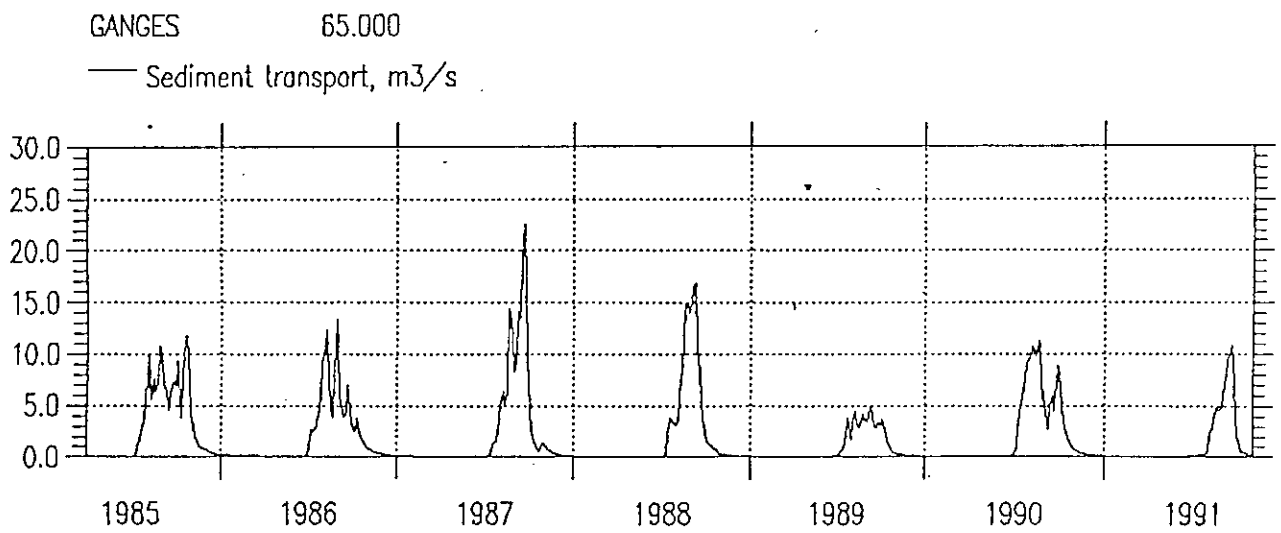
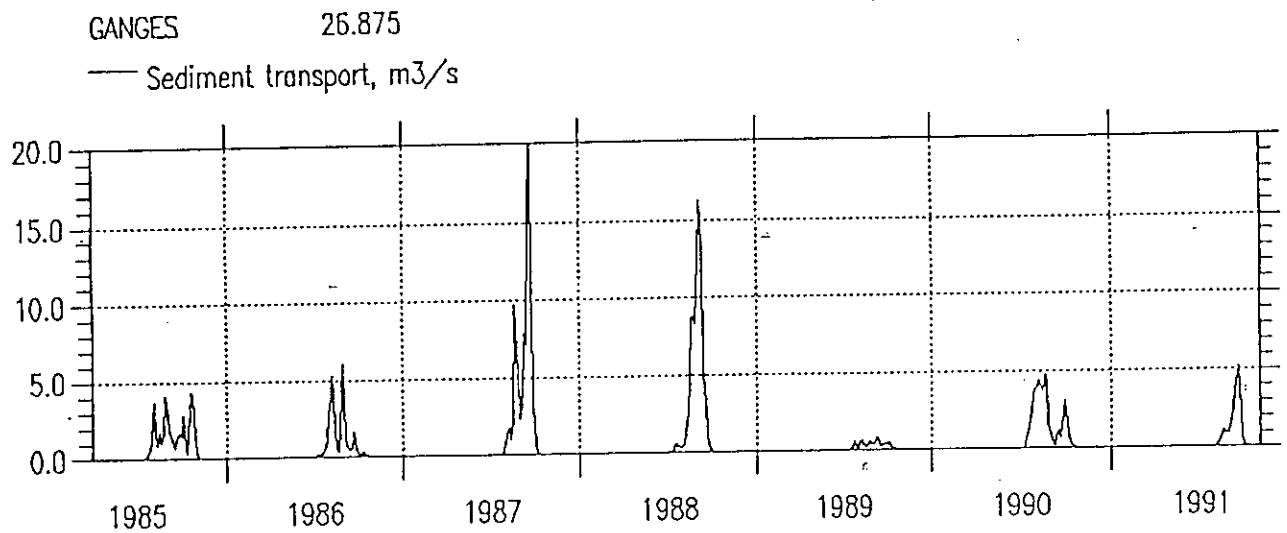


Figure 5.3 Computed sediment transport rate for the Ganges

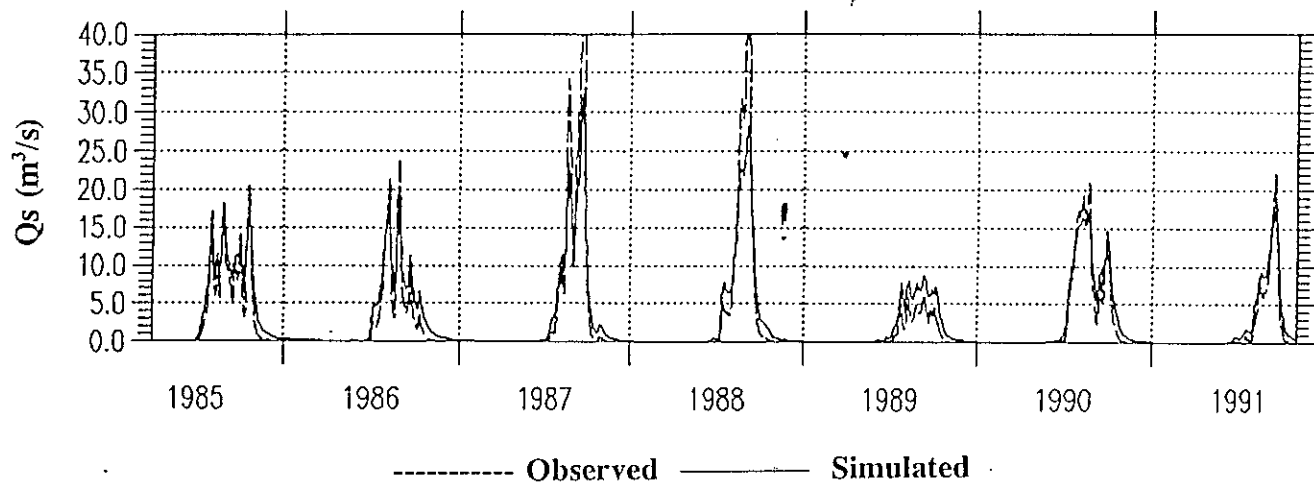


Figure 5.4 Observed and simulated sediment hydrographs at Hardinge Bridge

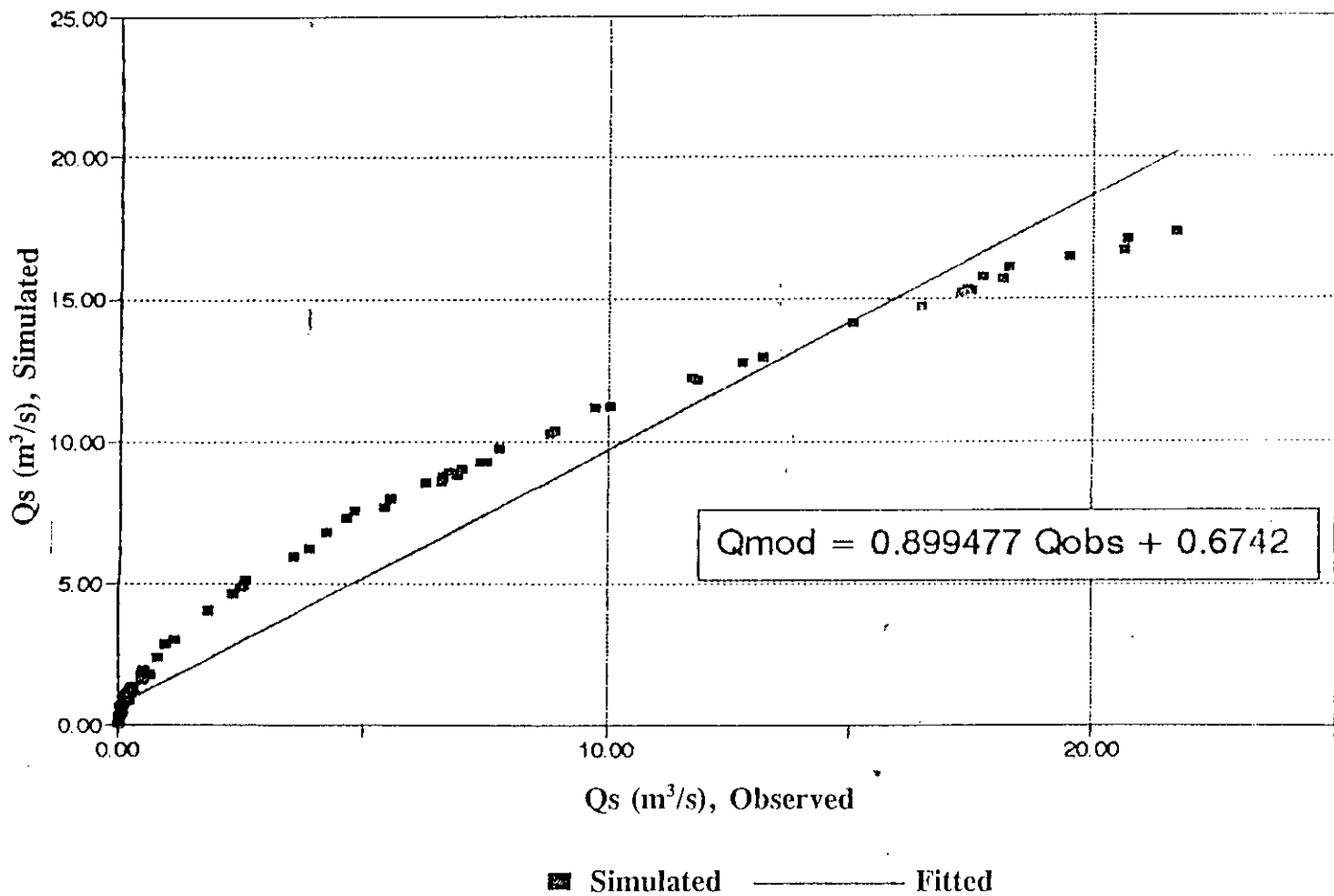


Figure 5.5 Comparison of simulated and observed transport rate (1990-91)

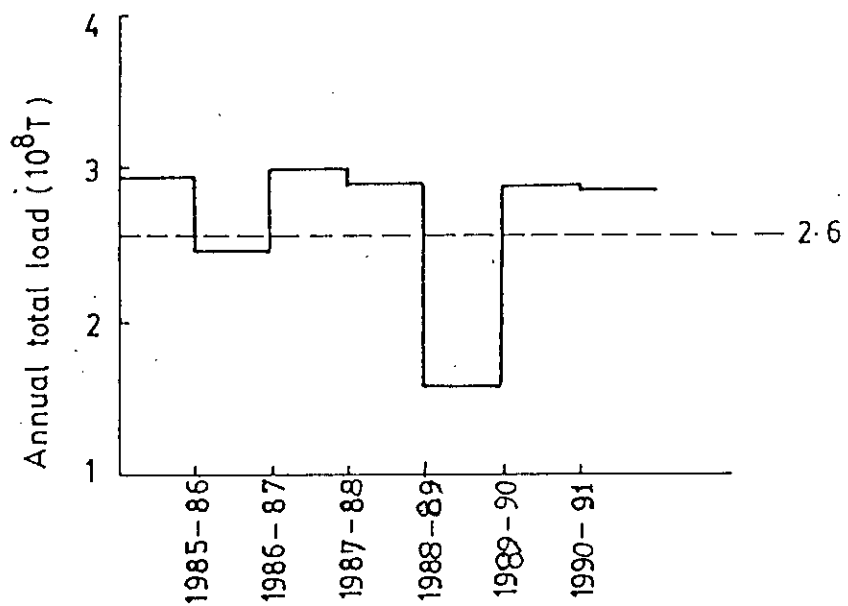
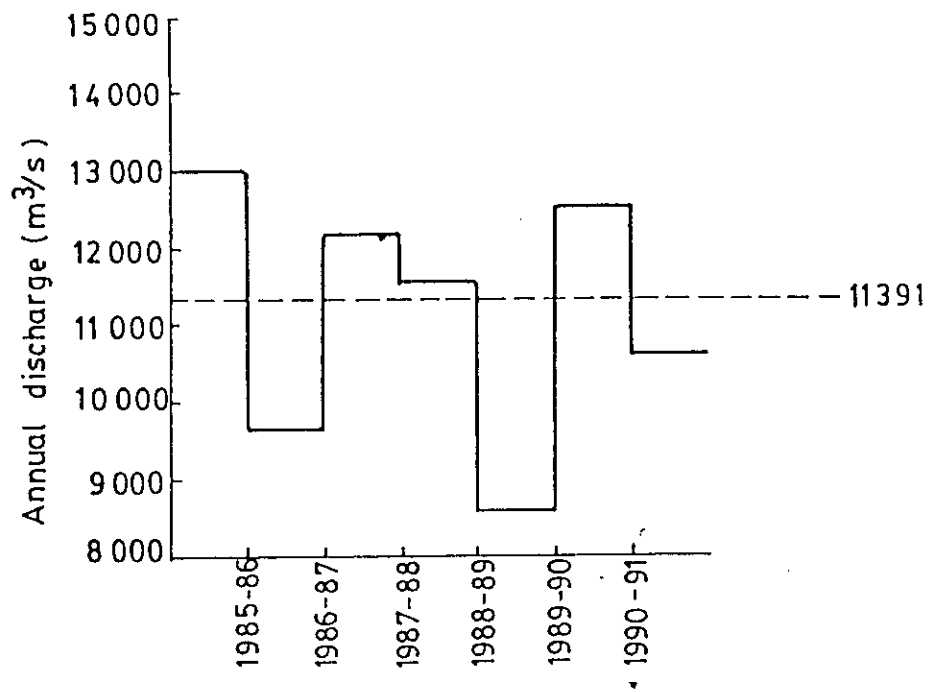


Figure 5.6 Variation of annual discharge and total load at Hardinge Bridge.

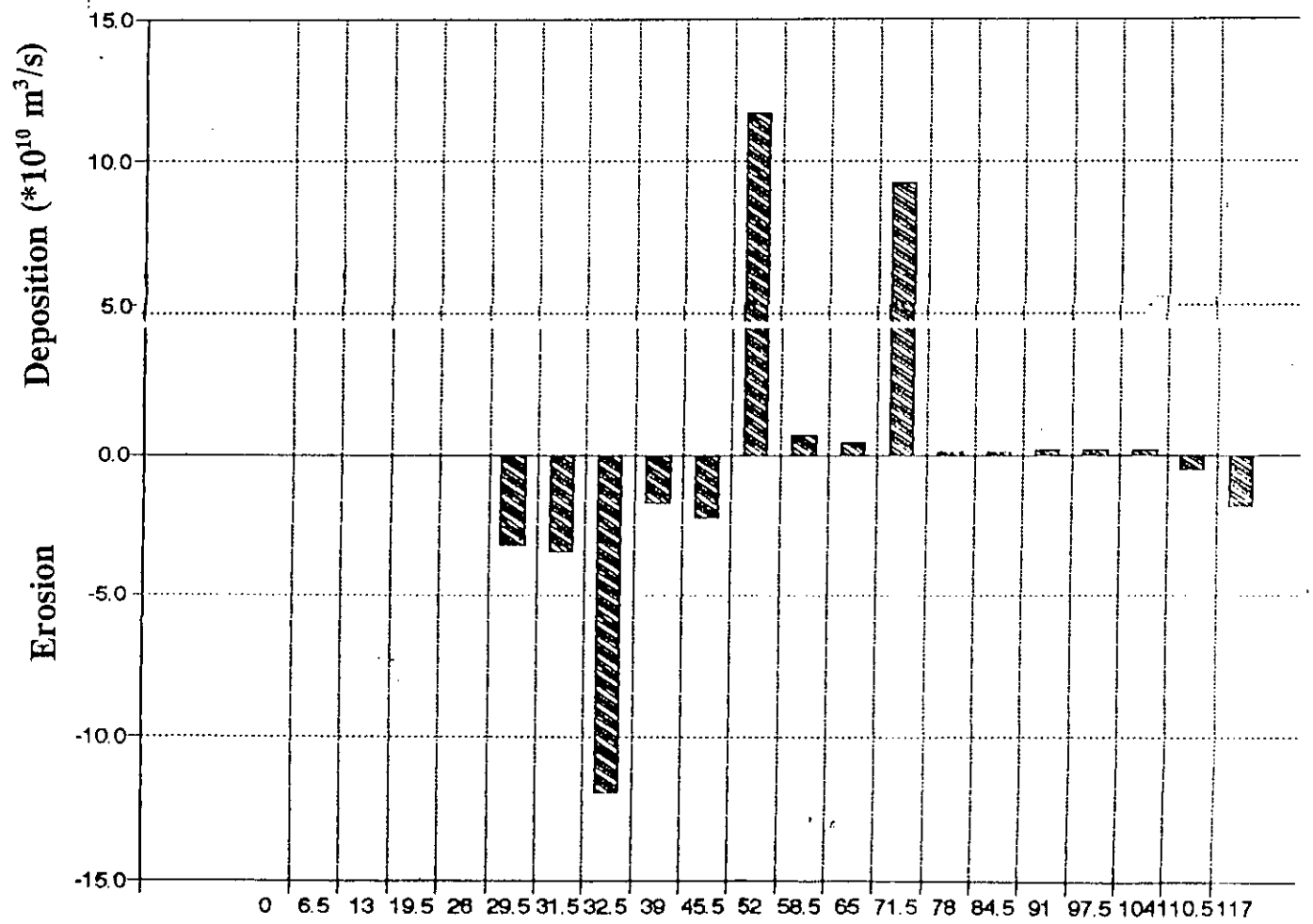


Figure 5.7 Distribution of degradation and aggradation along the Ganges

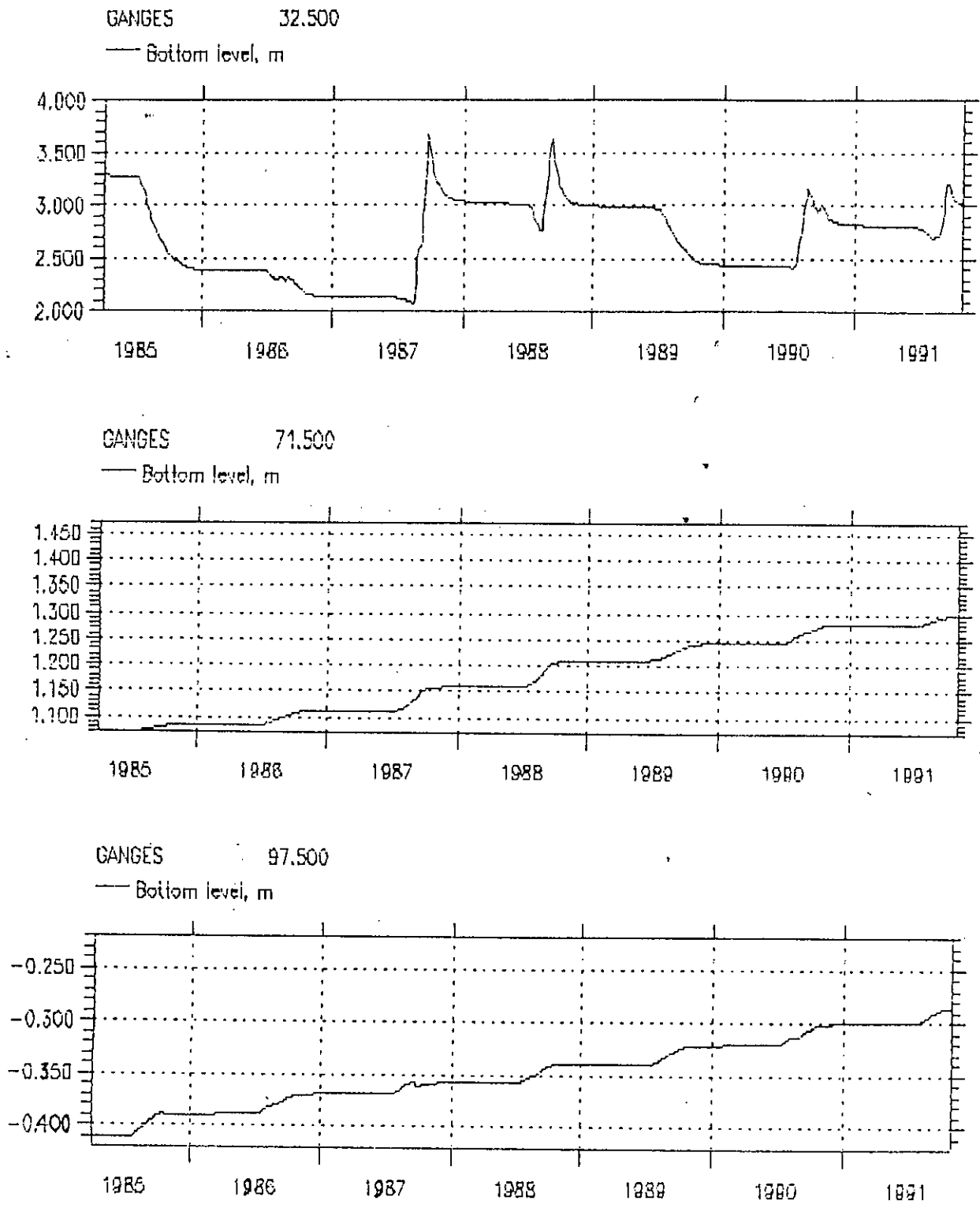


Figure 5.8 Variation of bed level at Hardinge Bridge, Sengram and Mohendrapur (1985-'91)

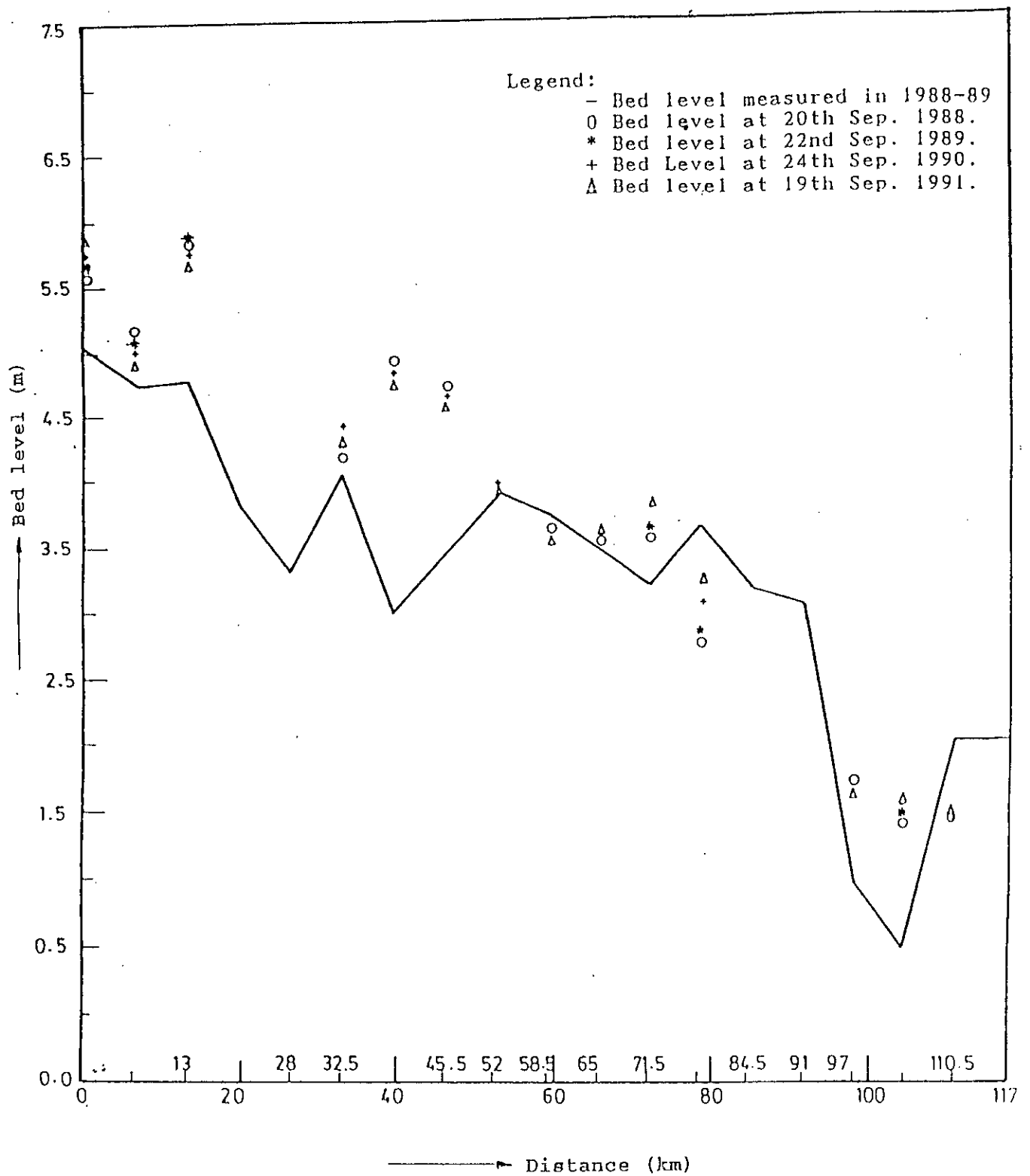


Figure 5.9 Variation of Bed Level along the River Reach.

CHAPTER VI

SUMMARY, CONCLUSIONS AND RECOMMENDATIONS

6.1 Summary

Engelund-Hansen equation has been used to simulate the sediment transport rates as well as update of bottom level for this study. One dimensional morphological module together with the hydrodynamic model have been used for this purpose. The actual cross-sections have been replaced with the equivalent cross-sections of the same hydraulic conditions. Both hydrodynamic and sediment boundary has been generated from the observed data after establishing rating curves. A representative grain size (D_{50}) has been used along the river reach from the gradation curves of bed material for the reach under study. The simulated results showed a good agreement with the observed values for transport rates, waterlevels and discharges. The model predicted the net amount of erosion and siltation along the river reach after each hydrodynamic computation.

6.2 Conclusions

The conclusions of this study may be summarized as follows:

(1) Applicability of transport equations have been studied with respect to the availability of the data as well as simplicity of the transport equations. It has been found that use of the Engelund-Hansen formulation will be reasonably good for the present situation.

(2) There exists an increasing trend of deposition of sediment in the Ganges after the Hardinge Bridge and this deposition trends reflects the change of bed level as shown in Figure 5.9.

(3) Overall, it is emphasized that MIKE11 one dimensional morphological model may not be useful for the river where bifurcation exists and for complicated network to simulate the actual variation of bed level changes.

6.3 Recommendations

(1) Input data should be analyzed thoroughly and modification should be done with some reliable extent to perform one dimensional morphological model run in combination with the hydrodynamic model.

(2) A sediment rating curve is established with the log-log regression for the observed transport rates of the Ganges and shown that the computed transport rates predicts well with the observed rates. Hence, rating parameter can be suggested where a long term field observations are available.

(3) For model calibration, multiplying factor (factor with a limit from 1.5 to 2.0) was not utilized in the observed transport rates while using of Engelund-Hansen formula. So, without using the calibration factors, the model can be used for some application with a reasonable limit of accuracy.

(4) Various sediment transport formulations can be used according to the availability of the field observations to select a more representative formulation for morphological study of a river.

(5) A difficulty exists while modelling sediment transport in a bifurcation especially in an one dimensional modelling. Because at the bifurcation there is no specific rule about the distribution of sediment. The division of sediment depends upon the three dimensional flow phenomenon at the bifurcation, which a one dimensional modelling approach can not take into account. So only a simple network can be taken in an one dimensional morphological model for future study of rivers where a large number of bifurcation exist in the rivers.

(6) Using this model, morphological impact can be characterized by (a) using a narrow section in the river reach with structures, (b) Increasing sediment input to the channel at the boundary, and (c) Rise in water level at the downstream boundary.

REFERENCES

1. Abbott, M.B.(1975), "Computational fluid dynamics, an introduction for engineers", Lecture notes, International Institute for Hydraulic and Environmental Engineering, Delft, the Netherland.
2. Ackers, P. and White, W.R.(1973), "Sediment transports, new approach and analysis", Proc. ASCE, JHD.99.HY11.
3. Alam, M.K. and Ahmed, S.M.(1980), "Peak flow analysis and evaluation of sediment transport capacity of the Ganges", UGC Research project, Department of Water Resources Engineering, BUET, Dhaka.
4. Bari, M.F.(1978), "Applicability of sediment transport formulas for the Ganges and Jamuna", M.Sc. Engineering Thesis, Department of Water Resources Engineering, BUET, Dhaka.
5. BWDB (1987), "Floods in Bangladesh", Ministry of Irrigation, Water Development and Flood Control, Bangladesh, December.
6. BWDB (1972), "Sediment investigation in main rivers of Bangladesh", BWDB water supply paper, No.359, Dhaka.
7. Chowdhury J.U.(1986), "An implicit numerical model of unsteady flow in river networks", Report No. R01/86, IFCDR, BUET, Dhaka.
8. Coleman, J.M. (1969), "Brahmaputra river, channel processes and sedimentation", Sedimentary geology, Vol.3.No.43,129-230.
9. CBJET (1991), "China Bangladesh joint expert team study", Final report, 1991.

10. Dad, M.M. (1977), "Study of river course shifting pattern in Bangladesh", M.Sc. Engineering Thesis, Department of Water Resources Engineering, BUET, Dhaka.
11. Engelund, F. and Hansen, E. (1967), "A monograph on sediment transport in alluvial streams", Teknisk Forlag, Copenhagen.
12. Engelund, F. (1966), "Hydraulic resistance of alluvial streams", ASCE, Vol. 92, No. HY2.
13. Engelund, F. and Fredsoe, J. (1976), "A Sediment transport model for straight alluvial channels", Nordic Hydrology, Vol. 7, No. 5.
14. Hossain, M.M. (1989), "Geomorphic characteristics of the Padma upto Brahmaputra confluence", Final report, R02/89.
15. Hossain, M.M. (1991), "Total sediment load in the lower Ganges and Jamuna", Paper presented at the 35th annual convention of the institution of Engineers, Bangladesh, Chittagong, March 8-11, 1991.
16. Habibullah, M. (1987), "Computer modelling of river channel changes in alluvial condition", First interim report, Analytical study of channel changes of the Brahmaputra, IFCDR, BUET, May 1987.
17. Hydraulic Research Laboratory, (1976), "Sediment testing report, Analysis of suspended sediment samples of the river Jamuna and Ganges", BWDB, Dhaka. Report No. 100.
18. Jansen, P. Ph, Bendegom, V.L, den Berg, Vries, M. De and Zanen, A (1979), "Principles of river engineering", Pitman, London.
19. Master Plan Organization, (MPO. 1987), "Surface water simulation modelling project", Interim Report II, Ministry of Irrigation, Water Development and Flood

Control, Bangladesh.

20. MIKE11 Reference Manual, Vol.2, "Transport dispersion, water quality, cohesive sediment transport, non-cohesive sediment transport", Danish Hydraulic Institute, Horsholm, Copenhagen.
21. Nahar (1991), "A numerical approach to study erosion deposition in a river reach", M.Sc, Engineering Thesis, Department of Water Resources Engineering, BUET, Dhaka.
22. Rijn, L.C. Van. (1984 a), "Part I : Bed load transport", J. Hyd, Eng., Vol No.110,10 October.
23. Rijn, L.C. Van.(1984 b), "Part II :Suspended load transport", J.Hyd. Eng,Vol No.110,11 November.
24. Rahman, K.S. (1978), "A study on the erosion of the river Padma", M.Sc. Engineering Thesis, Department of Water Resources Engineering, BUET, Dhaka.
25. River Research Institute,(1978), "Sediment testing report, Analysis of suspended sediment samples and bed material of the river Ganges and the Jamuna", BWDB, Report No.120.
26. River Research Institute,(1992), "Sediment testing report, Analysis of suspended sediment samples and bed material of the river Meghna in connection with Meghna river bank protection study (1992)", RRI, Faridpur.
27. Vries, M. de (1981), "Morphological computations", Lecture notes, (f10a, Delft University of Techn., Dept. of Civ.Eng., fluid Mech. Group, Delft, the Netherland.

